SUPPORTING INFORMATION FOR:

Calcium-catalysed ring-opening copolymerisation of epoxides and cyclic anhydrides

Enrique Francés-Poveda,[a] *Marc Martínez de Sarasa Buchaca,*[a] *Carmen Moya-López,*[b] *Iñigo J. Vitorica-Yrezabal,*[c] *Isabel López-Solera,*[a] *José A. Castro-Osma,*[b] *Felipe de la Cruz-Martínez,*[b,*] *Agustín Lara-Sánchez*[a,*]

[a]Universidad de Castilla-La Mancha, Departamento de Química Inorgánica, Orgánica y Bioquímica-Centro de Innovación en Química Avanzada (ORFEO-CINQA), Facultad de Ciencias y Tecnologías Químicas and Instituto Regional de Investigación Científica Aplicada-IRICA, 13071-Ciudad Real, Spain. E-mail: Agustin.Lara@uclm.es

[b]Universidad de Castilla-La Mancha, Departamento de Química Inorgánica, Orgánica y Bioquímica-Centro de Innovación en Química Avanzada (ORFEO-CINQA), Facultad de Farmacia and Instituto Regional de Investigación Científica Aplicada-IRICA, 02071-Albacete, Spain. E-mail: Felipe.Cruz@uclm.es

[c]Universidad de Granada, Departamento de Química Inorgánica, Facultad de Ciencias, 18071-Granada, Spain.

Table of Contents

1. Experimental section

1.1. General considerations

All manipulations of air and water sensitive compounds were carried out under dry nitrogen using a Braun Labmaster glovebox or standard Schlenk line techniques. NMR spectra were recorded on Bruker Ascend TM-500 spectrometer and referenced to the residual deuterated solvent. Microanalyses were carried out on a Perkin Elmer 2400 CHN analyzer. IR spectra were obtained on a Shimadzu IR Prestige-21 spectrophotometer equipped with a Pike Technology ATR system. MALDI-ToF analysis was carried out on a Bruker Autoflex III TOF/TOF spectrometer using dithranol (1,8,9-trihydroxyanthracene) as matrix material and NaI as additive. Gel permeation chromatography (GPC) measurements were performed on a Shimadzu LC-20A instrument equipped with a TSK-GEL G3000H column. The SEC column was eluted with THF at 25 °C at 1 mL·min^{-1} and was calibrated using eight monodisperse polystyrene standards in the range 580–48300 Da. TGA analysis was performed on a TA instrument TGA-Q50. The heating rate for the sample was 10 °C/min, and the nitrogen flow rate was 60 mL/min. DSC curves were obtained under N_2 atmosphere on a TA Instrument DSC-Q20. Samples were weighed into aluminum crucibles with 5 mg of sample and subjected to two heating cycles at a heating rate of 10 °C/min.

1.2. Materials

Solvents were pre-dried over sodium wire and distilled under nitrogen from sodium (toluene, *n*-hexane) or sodium/benzophenone (THF). Deuterated solvents were stored over activated 4 Å molecular sieves and degassed by several freeze-thaw cycles. Calcium iodide was purchased from Aldrich and used as received. Pro-ligands **L_2–L_4** were prepared according to literature procedures.[1] Cyclohexene oxide (CHO), 4-vinyl cyclohexene 1,2-epoxide (VCHO) and citraconic anhydride (CA) were dried overnight over CaH_2, fractionally distilled under reduced pressure and degassed. Methyl 9-(oxiran-2-yl)nonanoate (MUO) was prepared according to literature procedures[2] and dried over CaH_2. Phthalic anhydride (PA) was recrystallised from chloroform and sublimated under reduced pressure. All other reagents were purchased from common commercial sources and used as received.

1.3. Synthesis

1.3.1. Synthesis of protio-ligand L_1 and calcium complexes 1–4

Synthesis of protio-ligand bpzpeH (L_1): In a 250 mL Schlenk tube, bis(3,5-dimethyl-pyrazol-1-yl)methane (1.00 g, 4.89 mmol) was dissolved in dry THF (70 mL) and cooled to –70 °C. A solution of ^{n}BuLi (1.6 M in hexane, 3.06 mL, 4.89 mmol) was added, and the suspension was stirred for 1 h.

The mixture was warmed to −10 °C, and the resulting yellow suspension was added dropwise to a cooled (−10 °C) solution of benzaldehyde (0.50 mL, 4.89 mmol) in dry THF (20 mL). The mixture was stirred for 1 h and was allowed to warm up to ambient temperature. The product was hydrolysed with saturated aqueous NH_4Cl (15 mL). The organic layer was extracted, dried over $MgSO_4$ overnight and filtered, and the solvent was removed under vacuum to give the product as a white solid. Yield: 85% (1.29 g). Anal. Calcd for $C_{18}H_{22}N_4O$: C, 69.7; H, 7,1; N, 18.1. Found: C, 70.1; H, 7.3; N, 17.8. ^{1}H NMR (500 MHz, $CDCl_3$, 298 K): δ = 7.25–7.12 (m, 5H, Ph), 5.91–5.85 (m, 2H, CH, CH^a), 5.81 (s, 1H, H$^{4'}$), 5.60 (s, 1H, H^4), 5.10 (s, 1H, OH), 2.28 (s, 3H, Me^3), 2.17 (s, 3H, Me$^{3'}$), 1.93 (s, 3H, Me^5), 1.66 (s, 3H, Me$^{5'}$). ^{13}C NMR (126 MHz, $CDCl_3$, 298 K): δ = 148.9, 148.7, 140.7, 139.8, 138.4 (C$^{3,3',5,5'}$, ^{i}C-Ph), 128.3–126.8 (Ph), 106.8 (C$^{4'}$), 105.8 (C^4), 74.4, 74.3 (CH and CH^a), 13.9, 13.8 (Me$^{3,3'}$), 10.8, 10.4 (Me$^{5,5'}$).

Synthesis of [CaI{(κ^3-bpzpe)(μ-O)}(thf)]$_2$ (1): In a Schlenk tube, bpzpeH (**L$_1$**) (0.50 g, 1.05 mmol) was dissolved in dry THF (20 mL) and cooled down to −78 ºC. A solution of ^{n}BuLi (1.6 M in hexane, 0.65 mL, 1.05 mmol) was added dropwise and the mixture was maintained at −78 ºC for one hour. Then, the resulting solution was transferred to a pre-cooled slurry of CaI_2 (0.31 g, 1.05 mmol) in THF (20 mL). The reaction mixture was warmed to room temperature and left stirring overnight. A white solid precipitated, which was filtered and dried *in vacuo* to afford complex **1** in 78% yield (0.89 g). Suitable crystals for X-ray analysis were obtained from a CH_2Cl_2/*n*-hexane solution at room temperature. Anal. Calcd for $C_{44}H_{58}Ca_2I_2N_8O_4$: C, 48.2; H, 5.3; N, 10.2. Found: C, 48.4; H, 5.5; N, 10.0. ^{1}H NMR (500 MHz, $CDCl_3$, 298 K): δ = 7.34–7.18 (m, 10H, Ph), 6.46–5.44 (m, 8H, CH, CH^a, H$^{4,4'}$), 3.75 (m, 8H, thf), 2.74–1.36 (brs, 24H, Me$^{3,3'}$, Me$^{5,5'}$), 1.78 (m, 8H, thf). ^{13}C NMR (126 MHz, $CDCl_3$, 298 K): δ = 152.2–139.2 (C$^{3,3',5,5'}$,^{i}C-Ph), 129.8–124.4 (Ph), 109.0–105.3 (C$^{4,4'}$), 80.8, 80.1, 79.9, 78.8 (CH^a), 71.3, 70.1, 70.0 (CH), 68.8, 25.6 (thf), 17.3–10.3 (Me$^{3,3'}$, Me$^{5,5'}$).

Synthesis of [CaI{(κ^3-bpzFerr)(μ-O)}(thf)]$_2$ (2): The synthesis of **2** was carried out in an identical manner to **1**, using bpzFerrH (**L$_2$**) (0.50 g, 1.20 mmol), ^{n}BuLi (1.6 M in hexane, 0.82 mL, 1.20 mmol) and CaI_2 (0.35 g, 1.20 mmol). Compound **2** was isolated as a orange solid (70% yield, 1.10 g) and was recrystallised from a $CHCl_3$/*n*-hexane solution at room temperature. Anal. Calcd for $C_{52}H_{66}Ca_2Fe_2I_2N_8O_4$: C, 47.6; H, 5.1; N, 8.5. Found: C, 47.9; H, 5.3; N, 8.2. ^{1}H NMR (500 MHz, CD_3CN, 298 K): δ = 6.67, 6.34 (brs, 2H, CH), 5.95–5.77 (s, 4H, H$^{4,4'}$), 5.62, 5.41 (brs, 2H, CH^a), 4.71–3.67 (brs, 18H, Cp), 3.74 (m, 8H, thf), 2.50–1.90 (s, 24H, Me$^{3,3'}$, Me$^{5,5'}$), 1.77 (m, 8H, thf). ^{13}C{^{1}H} NMR (126 MHz, CD_3CN, 298 K): δ = 150.7–140.5 (C$^{3,3',5,5'}$), 107.4, 106.9, 106.8, 106.6

($C^{4,4'}$), 94.2, 93.8 (Cp), 76.7, 76.3 (CH^a), 71.3, 71.1, 70.4, 69.7, 69.5, 69.3, 68.3, 67.9, 67.5, 64.9, 64.7 (Cp, CH, thf), 26.2 (thf), 14.4, 14.3, 12.2, 11.9, 11.8, 11.7 ($Me^{3,3'}$, $Me^{5,5'}$).

Synthesis of [CaI{(κ^3-bpzbe)(μ-O)}(thf)]$_2$ (3): The synthesis of **3** was carried out in an identical manner to **1**, using bpzbeH (**L$_3$**) (0.50 g, 1.73 mmol), ^{n}BuLi (1.6 M in hexane, 1.18 mL, 1.73 mmol) and CaI_2 (0.50 g, 1.73 mmol). Compound **3** was isolated as a white solid (68% yield, 1.28 g). Anal. Calcd for $C_{40}H_{66}Ca_2I_2N_8O_4$: C, 45.5; H, 6.2; N, 10.6. Found: C, 45.7; H, 6.5; N, 10.4. ^{1}H NMR (500 MHz, CD_3CN, 298 K): δ = 6.27, 6.21 (s, 2H, CH), 6.00–5.74 (s, 4H, $H^{4,4'}$), 4.09, 4.05 (s, 2H, CH^a), 3.63 (m, 8H, thf), 2.46–2.25, 1.71 (s, 24H, $Me^{3,3'}$, $Me^{5,5'}$), 1.79 (m, 8H, thf), 0.84, 0.79 (s, 18H, ^{t}Bu). ^{13}C{^{1}H} NMR (126 MHz, CD_3CN, 298 K): δ = 149.9–139.5 ($C^{3,3',5,5'}$), 107.2, 107.1, 106.2, 106.0 ($C^{4,4'}$), 85.6, 84.7 (CH^a), 67.7 (CH, thf), 36.4, 35.8 (*C*-^{t}Bu), 27.0, 26.9 (*CH$_3$*-^{t}Bu), 25.6 (thf), 14.0, 13.7, 13.5, 11.4, 11.1, 10.9 ($Me^{3,3'}$, $Me^{5,5'}$).

Synthesis of [CaI{(κ^3-bpzbdeape)(μ-O)}(thf)]$_2$ (4): In a Schlenk tube, bpzdeapeH (**L$_4$**) (0.50 g, 0.94 mmol) was dissolved in dry THF (20 mL) and cooled down to −78 ºC. A solution of ^{n}BuLi (1.6 M in hexane, 0.58 mL, 0.94 mmol) was added dropwise and the mixture was maintained at −78 ºC for one hour. Then, the resulting solution was transferred to a pre-cooled slurry of CaI_2 (0.28 g, 0.94 mmol) in THF (20 mL). The reaction mixture was warmed to room temperature and left stirring overnight. The solvent was removed under vacuum affording a yellow solid, which was washed twice with *n*-hexane to give complex **4** as a white solid in 75% yield (1.08 g). Anal. Calcd for $C_{72}H_{102}Ca_2I_2N_{12}O_4$: C, 56.4; H, 6.7; N, 11.0. Found: C, 56.7; H, 6.9; N, 10.8. ^{1}H NMR (500 MHz, CD_3CN, 298 K): δ = 7.22 (m, 8H, ^{o}H-Ph), 6.59 (m, 8H, ^{m}H-Ph), 6.33 (s, 2H, CH), 5.74 (s, 4H, H^4), 3.63 (m, 8H, thf), 3.32 (m, 16H, N*CH$_2$*CH$_3$), 2.06, 2.03 (s, 24H, Me^3, Me^5), 1.79 (m, 8H, thf), 1.10 (m, 24H, NCH$_2$*CH$_3$*). ^{13}C{^{1}H} NMR (126 MHz, CD_3CN, 298 K): δ = 149.5, 147.1, 142.3 (C^3, C^5, ^{i}C-Ph), 133.3, 129.0, 111.4 (Ph), 105.9 (C^4), 73.6 (C^a, CH), 67.7 (thf), 44.3 (N*CH$_2$*CH$_3$), 25.6 (thf), 13.8, 11.3 (Me^3, Me^5), 12.3 (NCH$_2$*CH$_3$*).

1.3.2. Synthesis of polyesters

General polymerization procedure: In the glovebox, calcium catalyst (50.09 μmol, 0.1 equiv.), cyclic anhydride (5.09 mmol, 1.0 equiv.) and epoxide (5.09 mmol, 1.0 equiv.) were placed into a 25 mL Schlenk equipped with a small stir bar. Solvent (2 mL) were added to the reaction mixture. Then, the Schlenk was taken out of the glovebox, placed in a preheated oil bath under a nitrogen atmosphere at the desired temperature and kept stirring for the stated reaction time. The conversion of cyclic anhydride into the corresponding polyester was monitored by NMR. Once the polyester was obtained, the solvent was removed under vacuum. The resulting viscous mixture was dissolved in the minimum

amount of dichloromethane, precipitated with an excess of acidified methanol (1.0 M) and finally, filtered off and dried to afford the desired polymeric material.

Poly(CHO-*alt*-PA): Complex **4** (73 mg, 50.09 μmol), PA (754 mg, 5.09 mmol), CHO (500 mg, 5.09 mmol) and THF (2 mL) were sealed in a Schlenk and stirred for 24 h at 70 ºC. After that, the solvent was removed under vacuum. The resulting mixture was dissolved in CH_2Cl_2 and the polymer product precipitated from MeOH. The precipitate was filtered and dried under vacuum to afford the product as a white solid (1.06 g, 85 % yield). ^{1}H NMR (500 MHz, $CDCl_3$, 298 K) δ = 7.60 (2H, Ph), 7.41 (2H, Ph), 5.15 (2H, CH), 2,24–1.39 (8H, CH_2). ^{13}C NMR (126 MHz, $CDCl_3$, 298 K) δ = 166.8, 132.2, 131.2, 128.9, 74.8, 30.1, 23.6. **IR** (neat) υ(C=O) = 1716.34 cm^{-1}.

Poly(CHO-*alt*-CA): The synthesis of poly(CHO-*alt*-CA) was carried out in an identical manner to poly(CHO-*alt*-PA), using complex **4** (73 mg, 50.09 μmol), CA (570 mg, 5.09 mmol), CHO (500 mg, 5.09 mmol) and THF (2 mL). Poly(CHO-*alt*-CA) was obtained as a white solid (0.77 g, 72% yield). ^{1}H NMR (500 MHz, $CDCl_3$, 298 K) δ = 5.82–5.78 (1H, CH), 4.97–4.81 (2H, CH), 2.08–1.35 (11H, CH_2, Me). ^{13}C NMR (126 MHz, $CDCl_3$, 298 K) δ = 168.2, 165.1, 164.2, 146.6, 120.6, 79.5, 74.4, 73.9, 72.9, 32.7, 32.5, 30.2, 24.3, 24.1, 23.9, 23.5, 21.1, 20.7. **IR** (neat) υ(C=O) = 1729.41 cm^{-1}.

Poly(VCHO-*alt*-PA): The synthesis of poly(VCHO-*alt*-PA) was carried out in an identical manner to poly(CHO-*alt*-PA), using complex **4** (73 mg, 50.09 μmol), PA (754 mg, 5.09 mmol), VCHO (632 mg, 5.09 mmol) and THF (2 mL). Poly(VCHO-*alt*-PA) was obtained as a white solid (1.08 g,78 % yield). ^{1}H NMR (500 MHz, $CDCl_3$, 298 K) δ = 7.68 (2H, Ph), 7.50 (2H, Ph), 5.79 (1H, CH), 5.37, 5.25 (2H, CH), 5.14, 5.10, 5.03 (3H, CH), 2.50 (1H, CH), 1.99 (4H, CH_2), 1.68, 1.61 (2H, CH_2). ^{13}C NMR (126 MHz, $CDCl_3$, 298 K) δ = 166.3, 141.7, 132.3, 131.3, 129.1, 114.1, 72.0, 71.1, 35,3, 32.1, 26.7, 25.7. **IR** (neat) υ(C=O) = 1716.37 cm^{-1}.

Poly(VCHO-*alt*-CA): The synthesis of poly(VCHO-*alt*-CA) was carried out in an identical manner to poly(CHO-*alt*-PA), using complex **4** (73 mg, 50.09 μmol), CA (570 mg, 5.09 mmol), VCHO (632 mg, 5.09 mmol) and THF (2 mL). Poly(VCHO-*alt*-CA) was obtained as a white solid (0.78 g, 65% yield). ^{1}H NMR (500 MHz, $CDCl_3$, 298 K) δ = 5.82 (2H, CH), 5.03 (4H, CH), 2.42 (1H, CH), 2.04–1.61 (9H, CH_2, Me). ^{13}C NMR (126 MHz, $CDCl_3$, 298 K) δ = 168.7, 167.8, 164.5, 163.7, 146.1, 141.6, 120.5, 114.1, 71.8, 71.7, 71.6, 71.3, 70.7, 70.1, 35.4, 35.2, 32.1, 31.7, 26.5, 25.6, 25.4, 21.0, 20.7. **IR** (neat) υ(C=O) = 1719.23 cm^{-1}.

Poly(MUO-*alt*-PA): The synthesis of poly(MUO-*alt*-PA) was carried out in an identical manner to poly(CHO-*alt*-PA), using complex **4** (73 mg, 50.09 μmol), PA (754 mg, 5.09 mmol), MUO (1.09 g,

5.09 mmol) and THF (2 mL). Poly(MUO-*alt*-PA) was obtained as a yellow oil (1.01 g, 55% yield). ^{1}H NMR (500 MHz, $CDCl_3$, 298 K) δ = 7.70 (2H, Ph), 7.49 (2H, Ph), 5.41 (1H, CH), 4.51, 4.40 (2H, CH2), 3.66 (3H, Me), 2.28–1.28 (16H, CH_2). ^{13}C NMR (126 MHz, $CDCl_3$, 298 K) δ = 174.4, 167.1, 131.4, 129.2, 73.1, 66.1, 51.6, 34.2, 30.9, 29.5, 29.4, 29.3, 29.2, 25.2, 25.1. **IR** (neat) υ(C=O) = 1722.12 cm^{-1}.

Poly(MUO-*alt*-CA): The synthesis of poly(MUO-*alt*-CA) was carried out in an identical manner to poly(CHO-*alt*-PA), using complex **4** (73 mg, 50.09 μmol), CA (570 mg, 5.09 mmol), MUO (1.09 g, 5.09 mmol) and THF (2 mL). Poly(MUO-*alt*-CA) was obtained as a yellow oil (0.76 g, 46% yield). ^{1}H NMR (500 MHz, $CDCl_3$, 298 K) δ = 5.87 (1H, CH), 5.11 (1H, CH), 4.21 (2H, CH_2), 3.66 (3H, Me), 2.29–1.29 (19H, Me, CH_2). **IR** (neat) υ(C=O) = 1728.87 cm^{-1}.

1.4. DOSY calibration plots

A calibration plot was obtained through a series of DOSY analysis using standards with molecular weights ranging from 44.1 to 892.3 $g \cdot mol^{-1}$ and CD_3CN as solvent (Table S1). From the diffusion coefficients of the external standards, a linear calibration graphic was obtained by plotting log(D) versus log(MW) (Figure S1). Following DOSY analysis of the product, the diffusion coefficient found for the signals corresponding to complex **4** allowed an estimate of the molecular weight of the species present in solution. On the other hand, the molecular weight for complex **4** in d_8-THF solution was determined using the calibration plot previously reported by Williams and co-workers.[3]

Table S1. Diffusion coefficients (D) of standards in CD_3CN solution.

Compound	Log(D)	MW ($g \cdot mol^{-1}$)	Log(MW)
CD_3CN	–8.368	44.1	1.6441
$HN(SiMe_2H)_2$	–8.580	133.3	2.1250
$Ca[N(SiMe_3)_2]_2$	–8.735	360.2	2.5565
bpzbdeapeH (**L_4**)	–8.867	528.4	2.7229
$[\{Zn(\kappa^3\text{-bpzdeape})\}(\mu\text{-}O_2CCH_3)_3\{Zn(HO_2CCH_3)\}]^4$	–8.959	892.3	2.9505

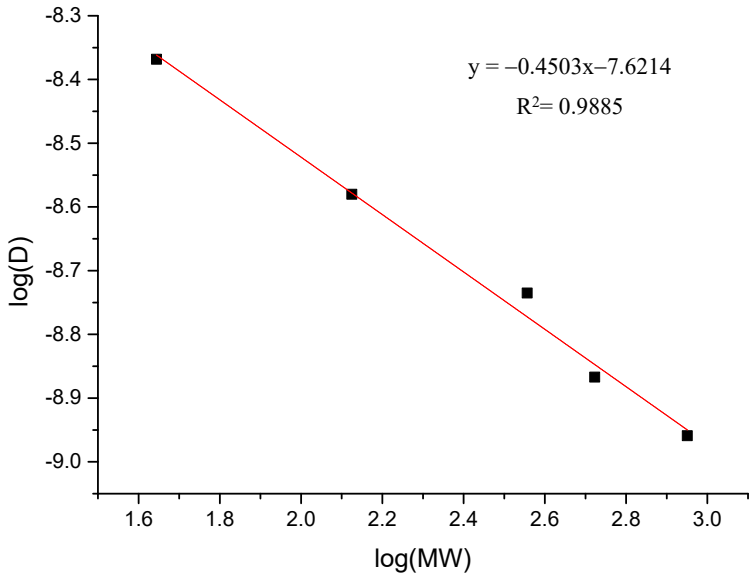

Figure S1. Plot of log(D) versus log(MW) from the DOSY NMR data obtained for different standards.

1.5. Kinetic analysis

1.5.1. Typical kinetic procedure

A representative procedure for the kinetic studies is described. In the glovebox, calcium catalyst, phthalic anhydride (PA), cyclohexene oxide (CHO) and a stock solution of mesitylene as internal standard were placed into a 25 mL Schlenk equipped with a small stir bar. THF was added to keep the total volume at 2 mL. Then, the Schlenk was taken out of the glovebox, placed in a preheated oil bath at 65 ºC under a nitrogen atmosphere and kept stirring. Small aliquots were taken at the desired times for NMR analysis to determine monomer conversions.

1.5.2. Initial rate determination

Reactions orders were determined by examining initial reaction rates (up to 20% completion) following the procedure described by Tolman and co-workers.[5] Table S2 collects a summary of the determined orders.

Table S2. Determined orders for CHO, PA and catalyst **4** using initial rates.

	CHO	PA	Catalyst **4**
Reaction order	0.1(3)	1.0(1)	0.5(1)

1.6. X-ray crystallographic structure determination

Suitable single crystals of complexes **1** and **1'** were mounted on a Bruker VENTURE diffractometer equipped with a PHOTON 3 detector, graphite monochromated Mo K_α radiation ($\lambda = 0.71073$ Å) and an Oxford cryosystem. 150 K single crystal X-ray diffraction data were collected and processed using APEX III software. Adsorption correction was applied using SADABS software by empirical methods measuring symmetry equivalent reflections at different azimuthal angles. All structures were solved using the SHELXT program and refined using least squares refinement methods on all F^2 values as implemented within SHELXL.[6] Both SHELXT and SHELXL were operated through the Olex2 (v1.5) interface.[7] All atoms were refined anisotropic and atomic displacement parameters were refined with suitable restraints applied to keep them physically reasonable. Hydrogen atoms were placed in calculated positions and refined with idealised geometries and assigned fixed occupancies and isotropic displacement parameters.

CCDC 2332643 and 2341168 contain the supplementary crystallographic data for this paper. These data can be obtained free of charge via www.ccdc.cam.ac.uk/data_request/cif, or by emailing data_request@ccdc.cam.ac.uk, or by contacting The Cambridge Crystallographic Data Centre, 12 Union Road, Cambridge, CB2 1EZ, UK; fax: +44 1223 336033. e-mail: deposit@ccdc.cam.ac.uk or http://www.ccdc.cam.ac.uk

2. Figures and Tables referred to in main text

Table S3. Crystal data and structure refinement for compounds **1** and **1'**

	Compound 1	**Compound 1'**
Empirical formula	$C_{44}H_{58}Ca_2I_2N_8O_4 \cdot 2CH_2Cl_2 \cdot 1/2C_6H_{14}$	$C_{36}H_{46}Ca_2I_2N_8O_4 \cdot 2CH_2Cl_2$
Formula weight	1309.88	1158.62
Temperature (K)	150(2)	296(2)
Wavelength (Å)	0.71073	0.71073
Crystal system	Monoclinic	Triclinic
Space group	$P2_1/c$	$P\bar{1}$
a(Å)	12.835(2)	9.505(3)
b(Å)	17.351(3)	10.990(3)
c(Å)	26.132(5)	12.918(5)
α(°)	90	106.384(11)
β(°)	95.473(6)	100.446(11)
γ(°)	90	93.892(10)
Volume(Å^3)	5793.1(17)	1263.0(7)
Z	4	1
Density (calculated) (g/cm^3)	1.502	1.523
Absorption coefficient (mm^{-1})	1.495	1.703
F(000)	2660	580
Crystal size (mm^3)	0.22 x 0.18 x 0.16	0.18 x 0.12 x 0.10
Index ranges	$-12 \le h \le 15$ $-20 \le k \le 20$ $-31 \le l \le 31$	$-11 \le h \le 11$ $-13 \le k \le 13$ $-16 \le l \le 16$
Reflections collected	67749	29978
Independent reflections	10522 [R(int) = 0.0732]	5188 [R(int) = 0.0762]
Data / restraints / parameters	10522 / 44 / 619	5188 / 0 / 270
Goodness-of-fit on F^2	1.145	1.031
Final R indices [$I>2\sigma(I)$]	R1 = 0.1078, wR2 = 0.2780	R1 = 0.0444, wR2 = 0.1230
Largest diff. peak / hole, e.Å^{-3}	1.50/-1.82	0.85/-1.15

Table S4. Selected bond distances (Å) and angles (°) for compounds **1** and **1'**

Compound 1		**Compound 1'**	
Ca(1)–I(1)	3.129(3)	Ca(1)–I(1)	3.1161(11)
Ca(1)–O(1)	2.244(9)	Ca(1)–O(1)	2.245(3)
Ca(1)–O(2)	2.282(9)	Ca(1)–O(2)	2.397(3)
Ca(1)–O(3)	2.360(10)	Ca(1)–O(1a)	2.273(3)
Ca(1)–N(1)	2.496(11)	Ca(1)–N(1)	2.527(3)
Ca(1)–N(2)	2.534(11)	Ca(1)–N(3)	2.471(3)
O(1)–Ca(1)–I(1)	105.1(2)	O(1)–Ca(1)–I(1)	177.26(7)
O(1)–Ca(1)–O(2)	80.5(3)	O(1)–Ca(1)–O(2)	97.31(12)
O(1)–Ca(1)–O(3)	162.6(3)	O(1)–Ca(1)–O(1a)	79.77(10)
O(1)–Ca(1)–N(1)	81.6(3)	O(1)–Ca(1)–N(1)	79.14(10)
O(1)–Ca(1)–N(2)	75.3(3)	O(1)–Ca(1)–N(3)	74.95(11)
O(2)–Ca(1)–I(1)	98.4(2)	O(1a)–Ca(1)–I(1)	100.79(7)
O(2)–Ca(1)–O(3)	103.1(3)	O(1a)–Ca(1)–O(2)	92.68(12)
O(2)–Ca(1)–N(2)	95.1(3)	O(1a)–Ca(1)–N(3)	92.06(11)
O(2)–Ca(1)–N(1)	160.0(3)	O(1a)–Ca(1)–N(1)	157.50(10)
O(3)–Ca(1)–I(1)	91.4(2)	O(2)–Ca(1)–I(1)	85.35(10)
O(3)–Ca(1)–N(2)	87.4(3)	O(2)–Ca(1)–N(3)	170.05(12)
O(3)–Ca(1)–N(1)	91.4(2)	O(2)–Ca(1)–N(1)	97.67(13)
N(2)–Ca(1)–I(1)	166.4(3)	N(3)–Ca(1)–I(1)	102.33(8)
N(1)–Ca(1)–I(1)	95.0(3)	N(1)–Ca(1)–I(1)	99.92(8)
N(1)–Ca(1)–N(2)	71.6(3)	N(1)–Ca(1)–N(3)	74.96(12)

Figure S2. Molecular structure of compound **1'**. Hydrogen atoms have been excluded for clarity. Thermal ellipsoids are set at 30% probability.

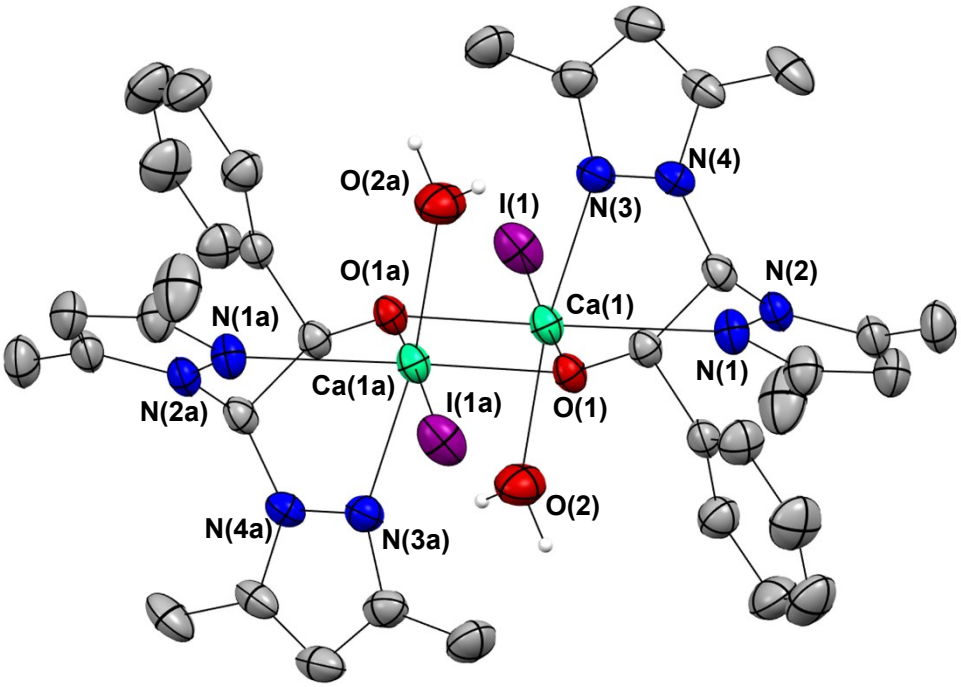

Figure S3. NMR spectra (500 MHz, $CDCl_3$, 298 K) of bpzpeH ($\mathbf{L_1}$)

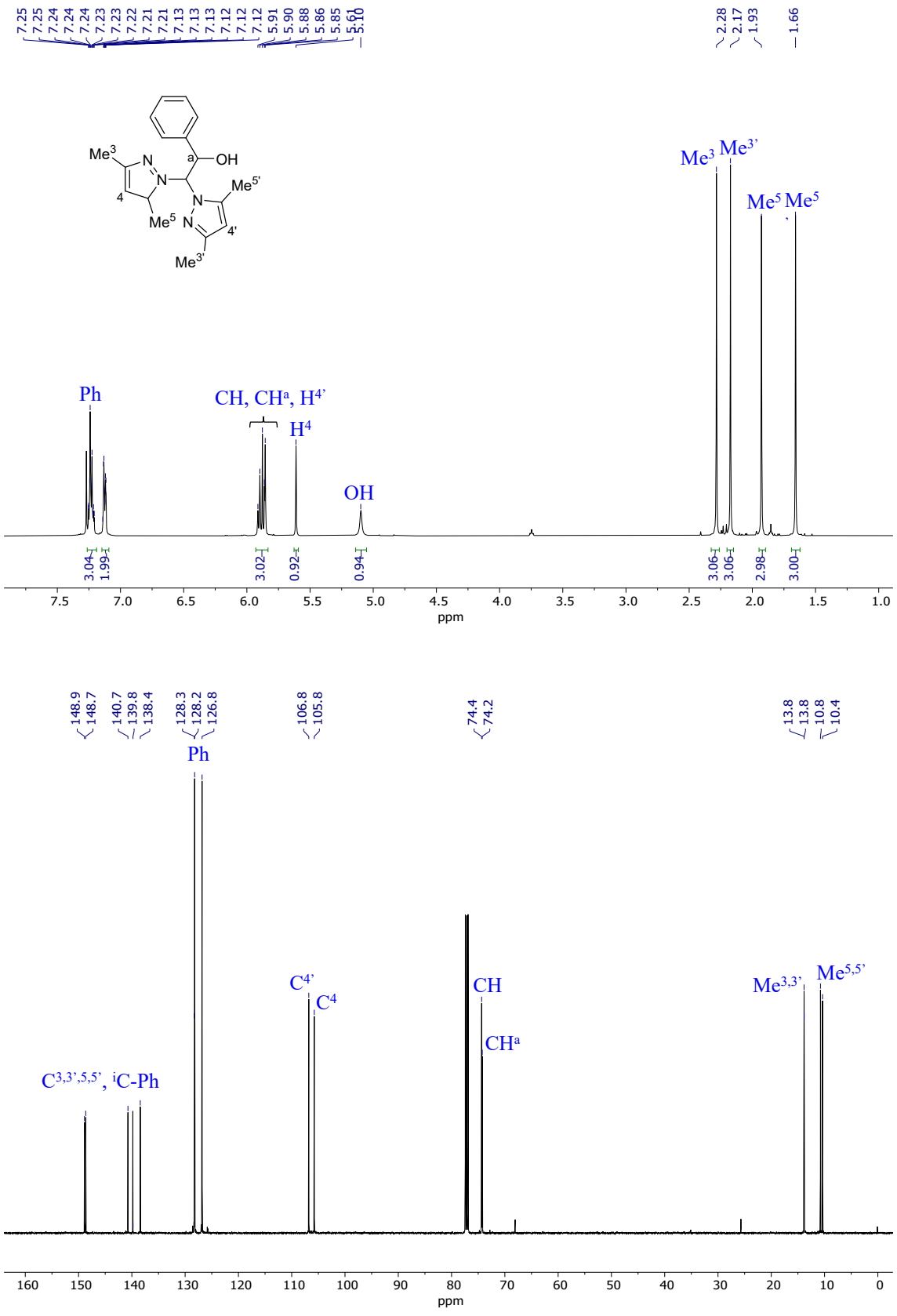

Figure S4. NMR spectra (500 MHz, $CDCl_3$, 298 K) of [CaI{(κ^3-bpzpe)(μ-O)}(thf)]$_2$ (**1**)

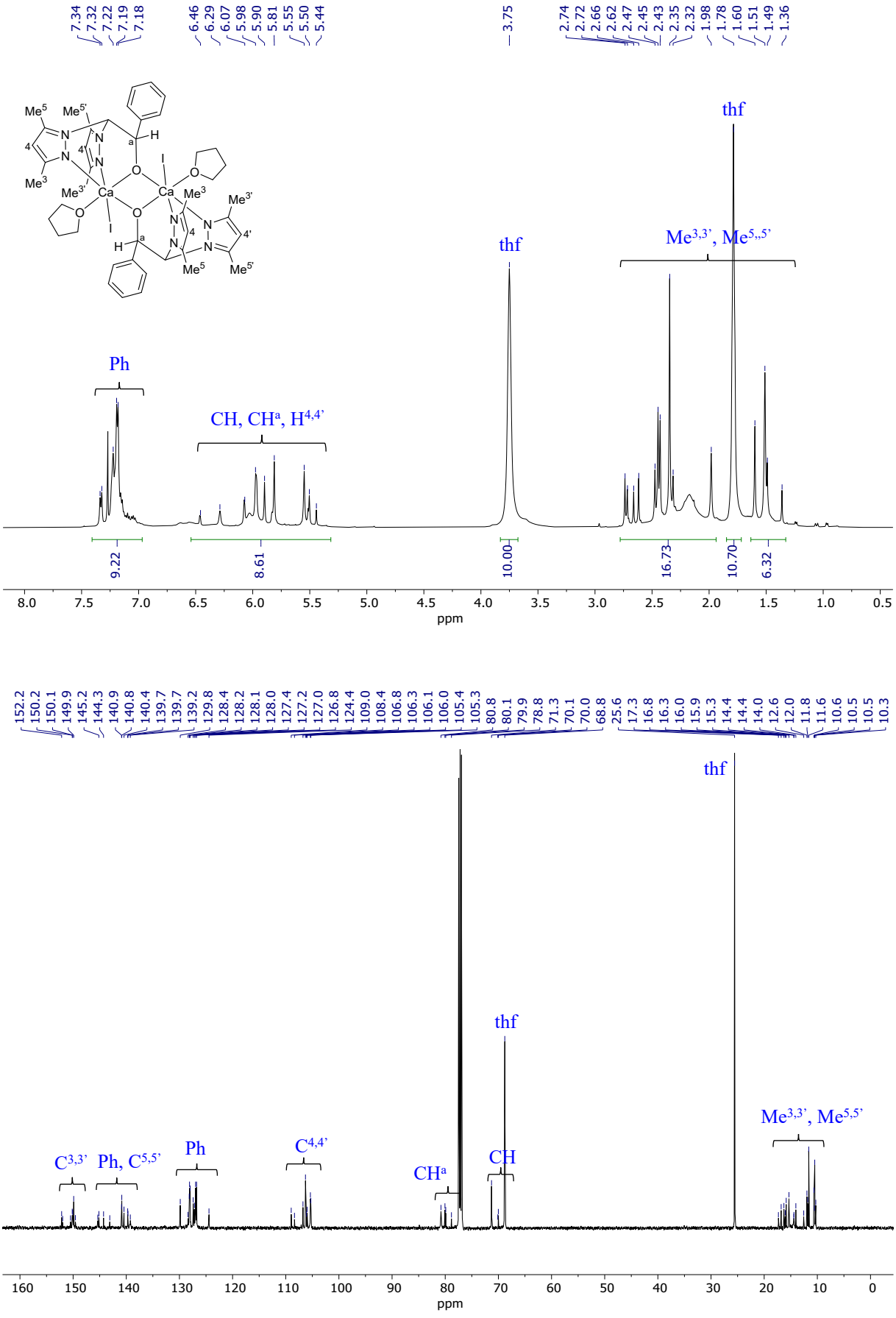

Figure S5. NMR spectra (500 MHz, CD_3CN, 298 K) of [CaI{(κ^3-bpzFerr)(μ-O)}(thf)]$_2$ (**2**)

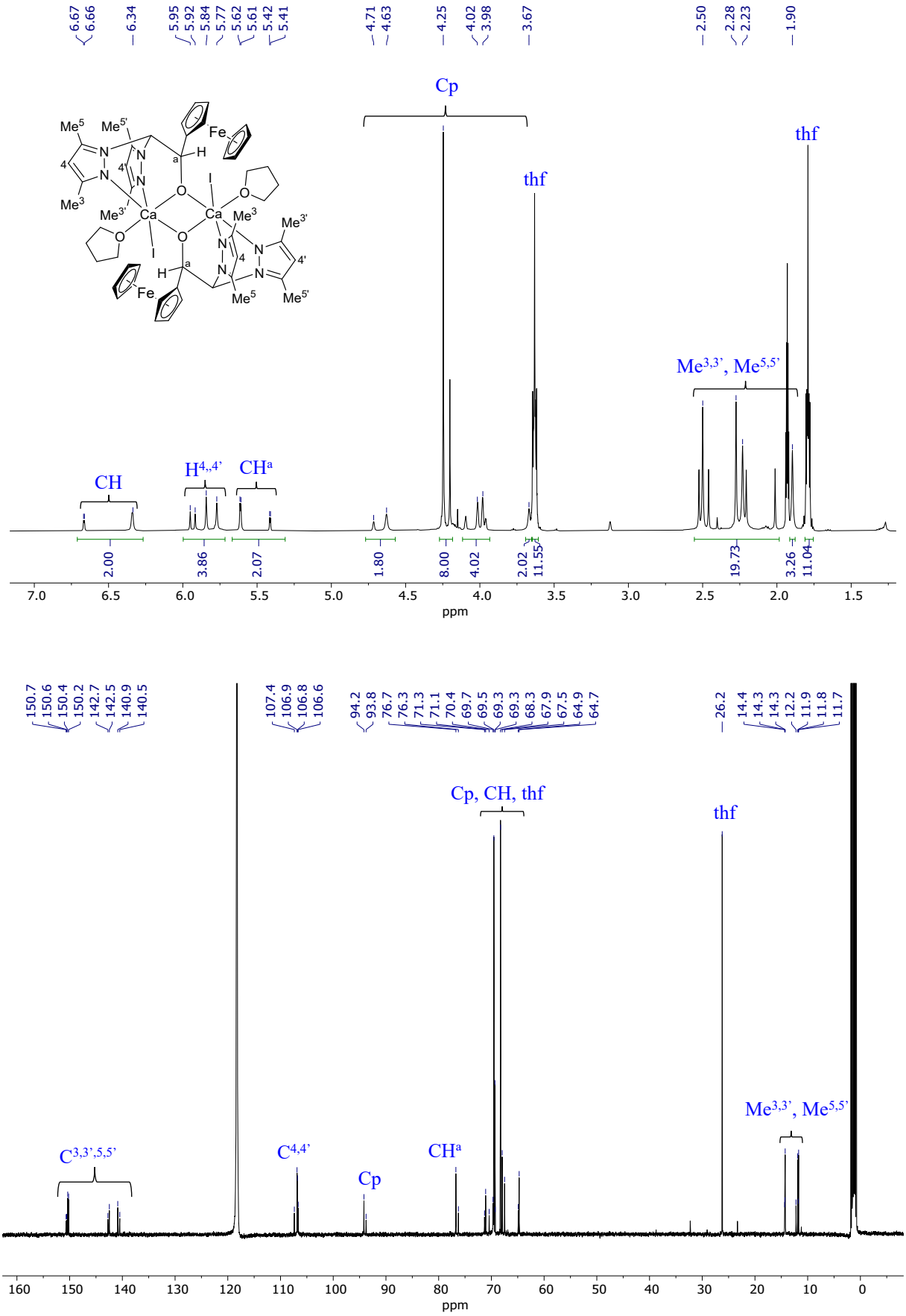

Figure S6. NMR spectra (500 MHz, CD_3CN, 298 K) of [CaI{(κ^3-bpzbe)(μ-O)}(thf)]$_2$ (**3**)

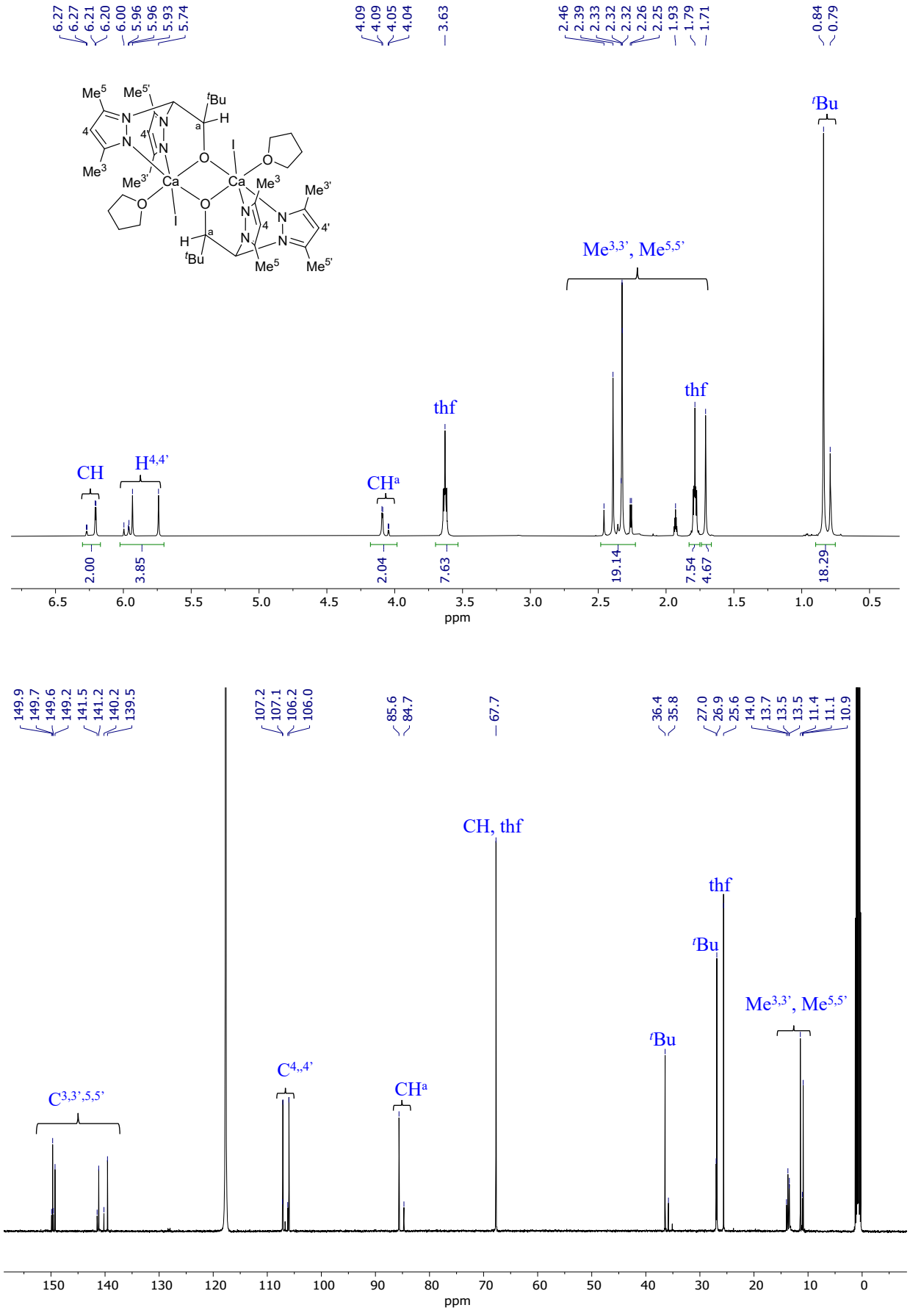

Figure S7. NMR spectra (500 MHz, CD_3CN, 298 K) of [CaI{(κ^3-bpzbdeape)(μ-O)}(thf)]$_2$ (**4**)

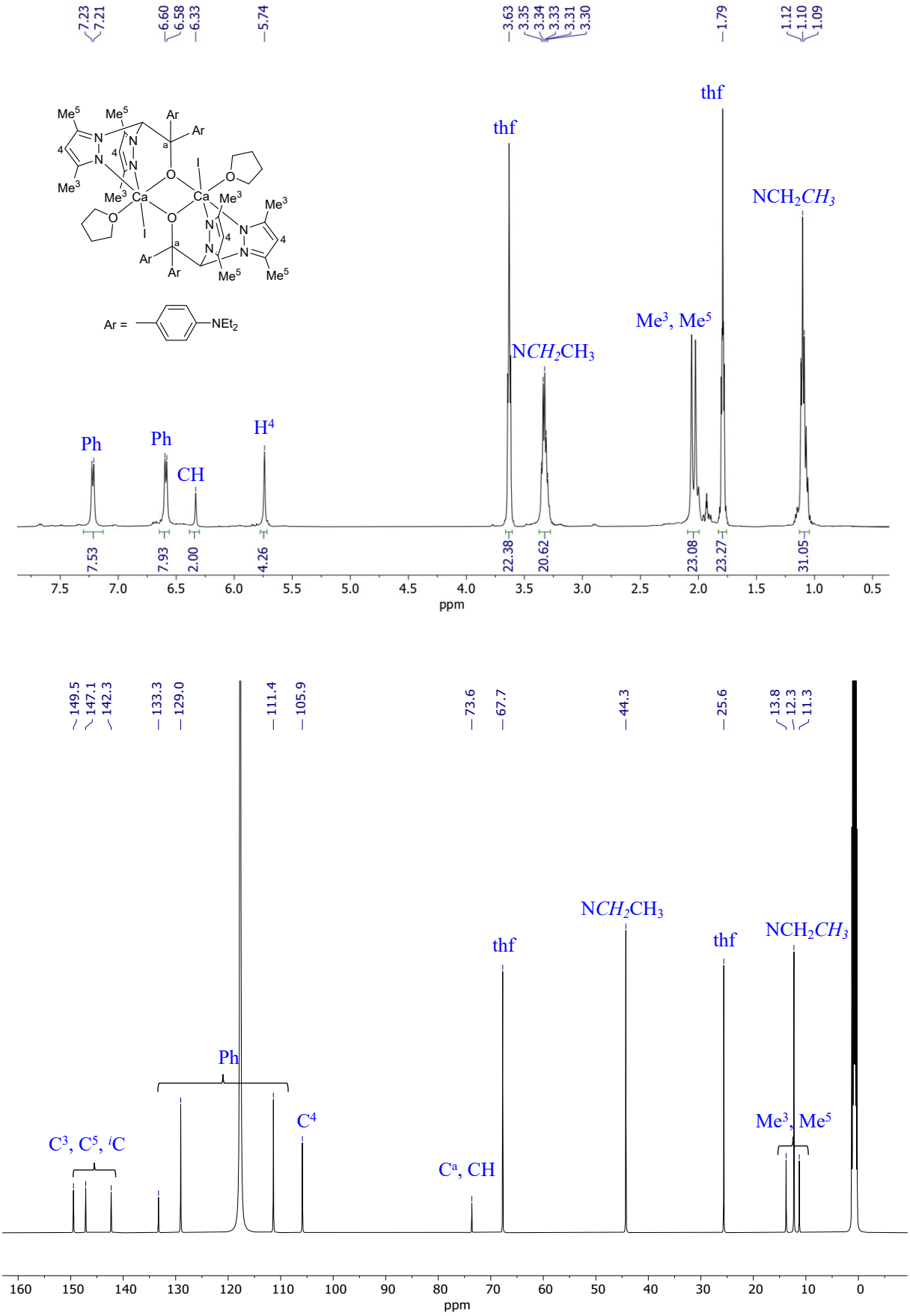

Figure S8. DOSY NMR analysis (500 MHz, CD_3CN, 298 K) of compound **4**.

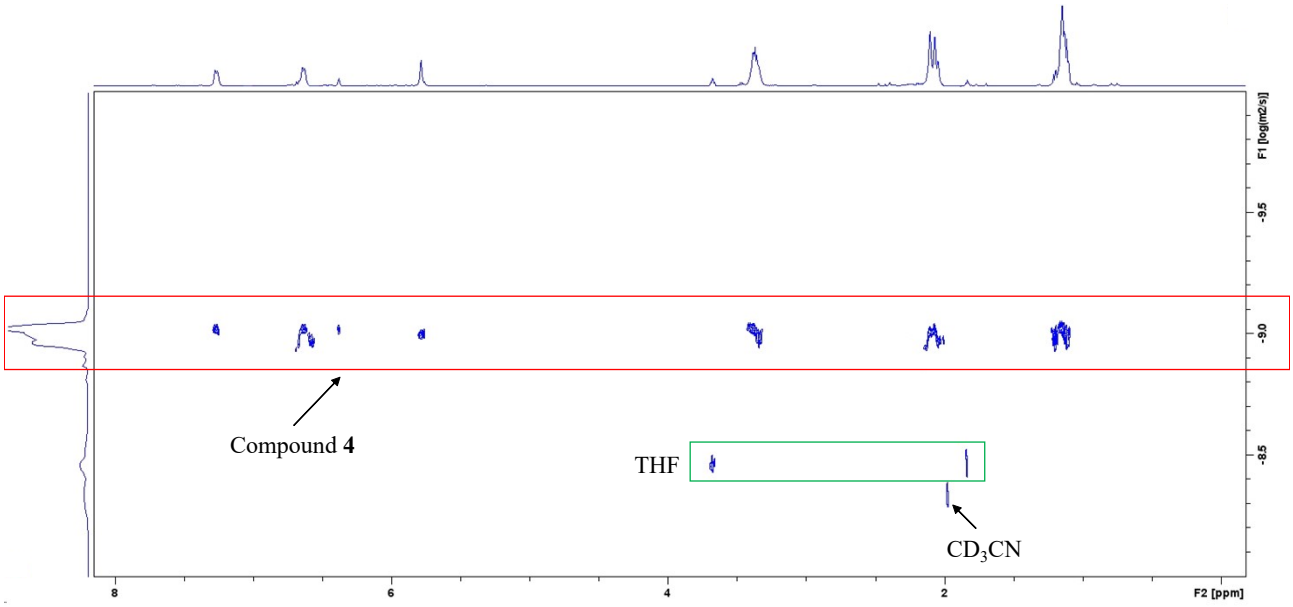

Figure S9. Representative SEC traces obtained for polyesters catalysed by compound **4**: a) Table 2, entry 2; b) Table 2, entry 4; c) Table 2, entry 6.

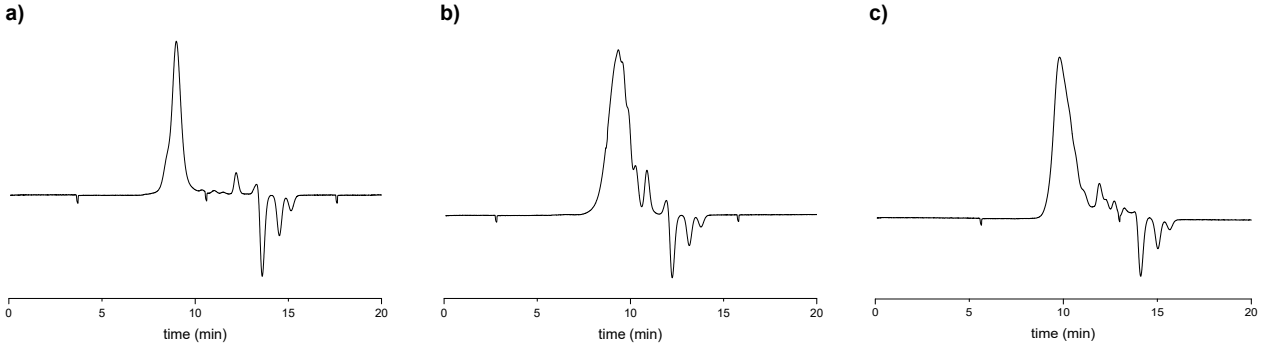

poly(CHO-*alt*-CA), Table 2, entry 2

M_n = 4.0 kg·mol^{-1}, *Đ* = 1.2

poly(VCHO-*alt*-CA), Table 2, entry 4

M_n = 3.3 kg·mol^{-1}, *Đ* = 1.4

poly(MUO-*alt*-CA), Table 2, entry 6

M_n = 2.3 kg·mol^{-1}, *Đ* = 1.4

Figure S10. NMR spectra (500 MHz, $CDCl_3$, 298 K) of poly(CHO-*alt*-PA)

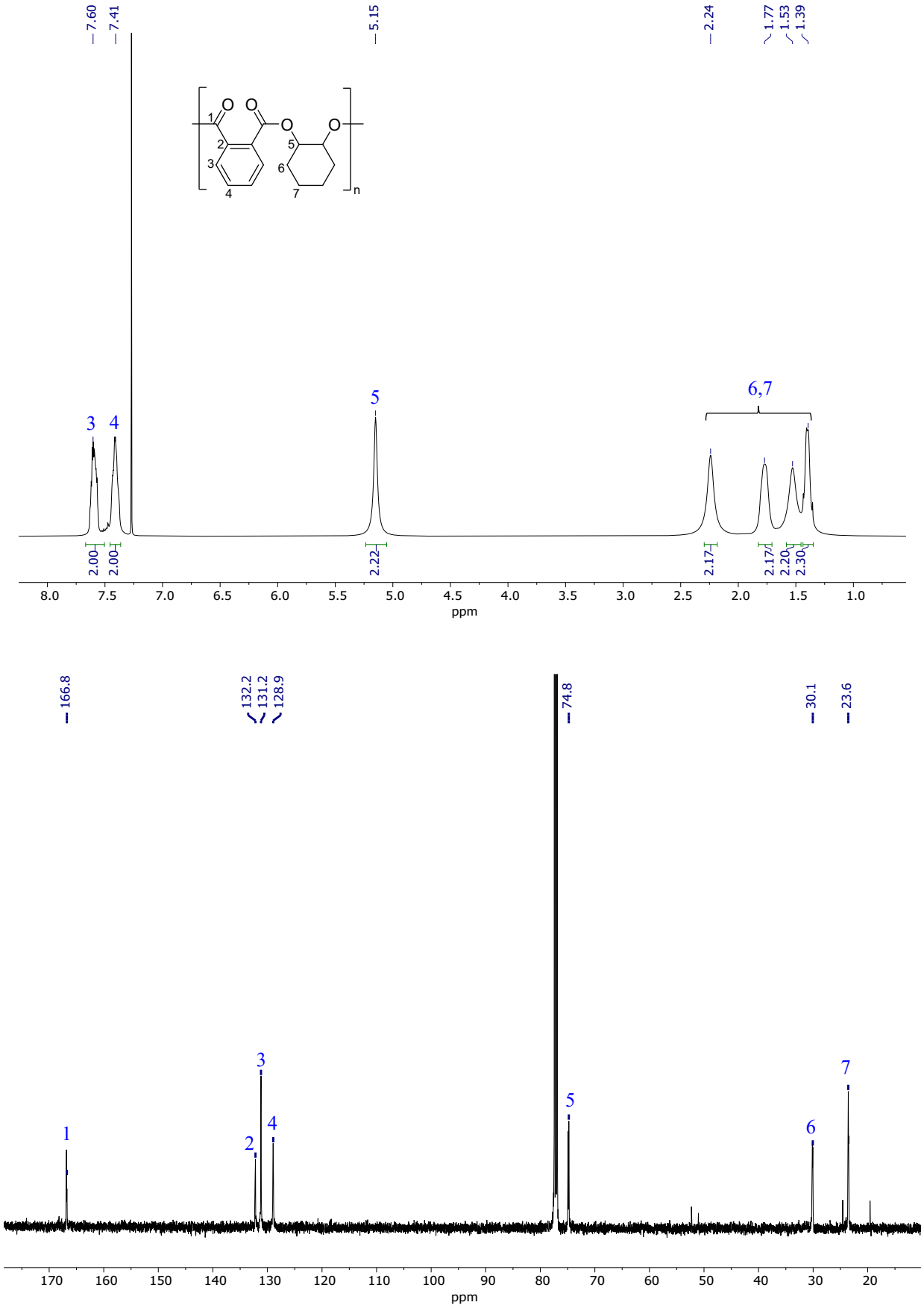

Figure S11. IR spectrum of poly(CHO-*alt*-PA)

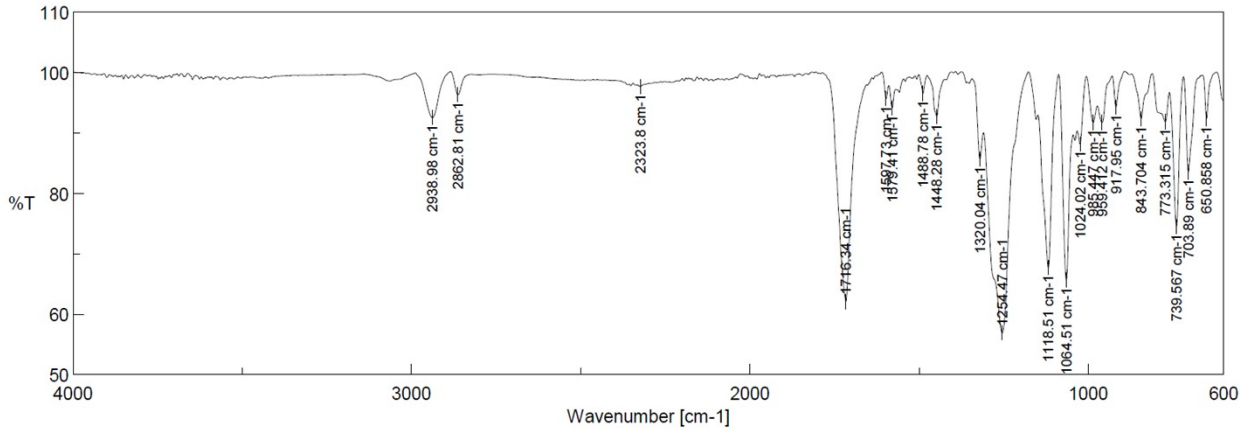

Figure S12. NMR spectra (500 MHz, $CDCl_3$, 298 K) of poly(CHO-*alt*-CA)

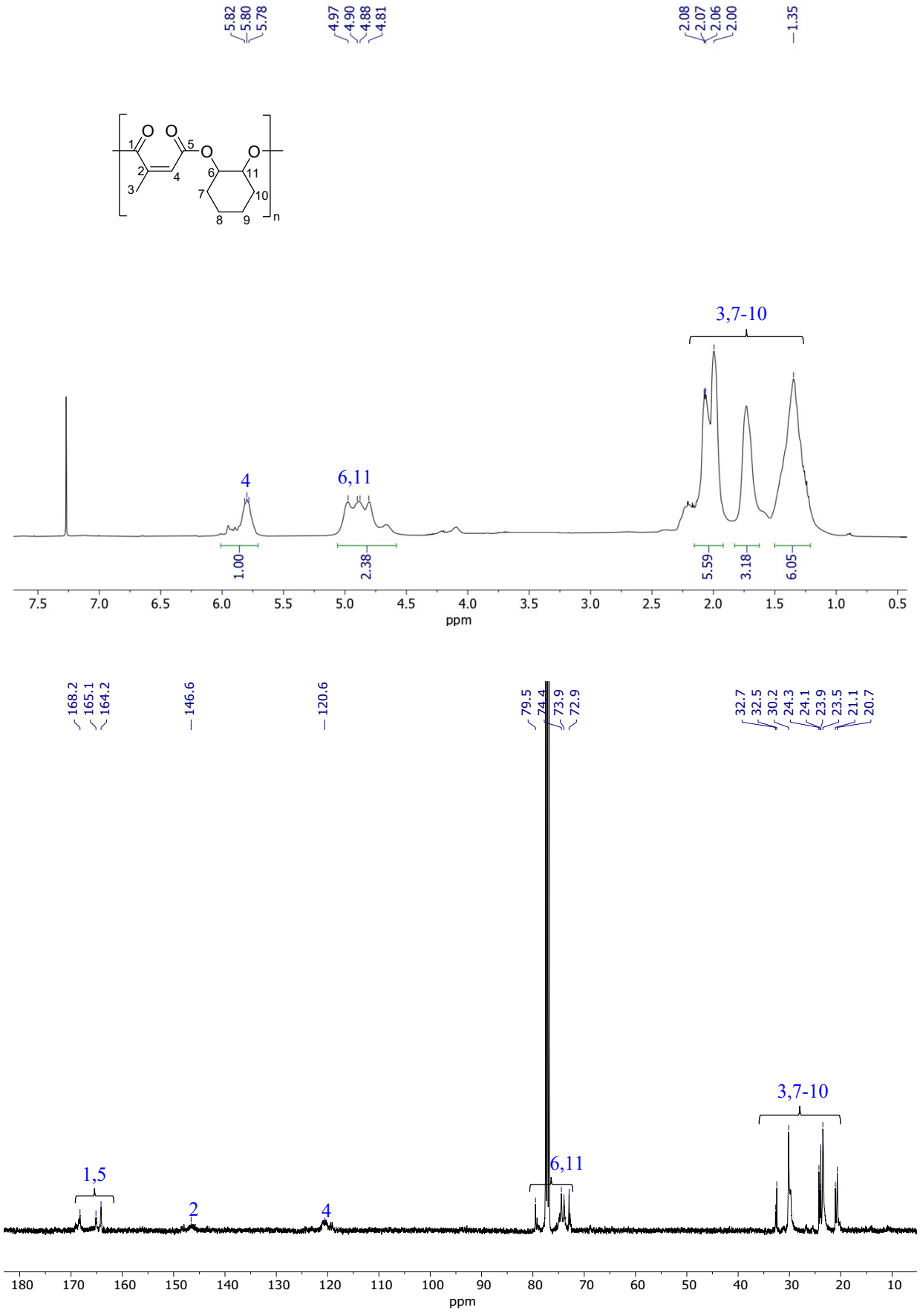

Figure S13. IR spectrum of poly(CHO-*alt*-CA)

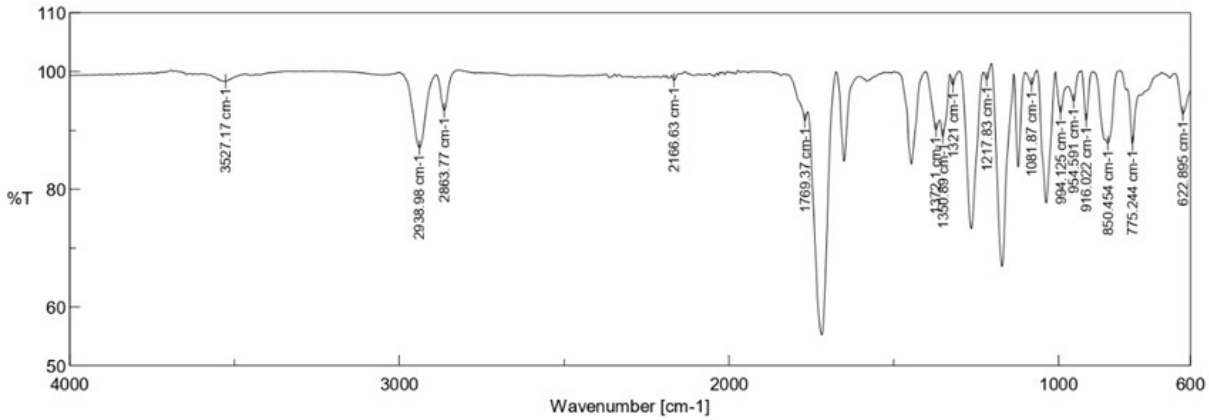

Figure S14. NMR spectra (500 MHz, $CDCl_3$, 298 K) of poly(VCHO-*alt*-PA)

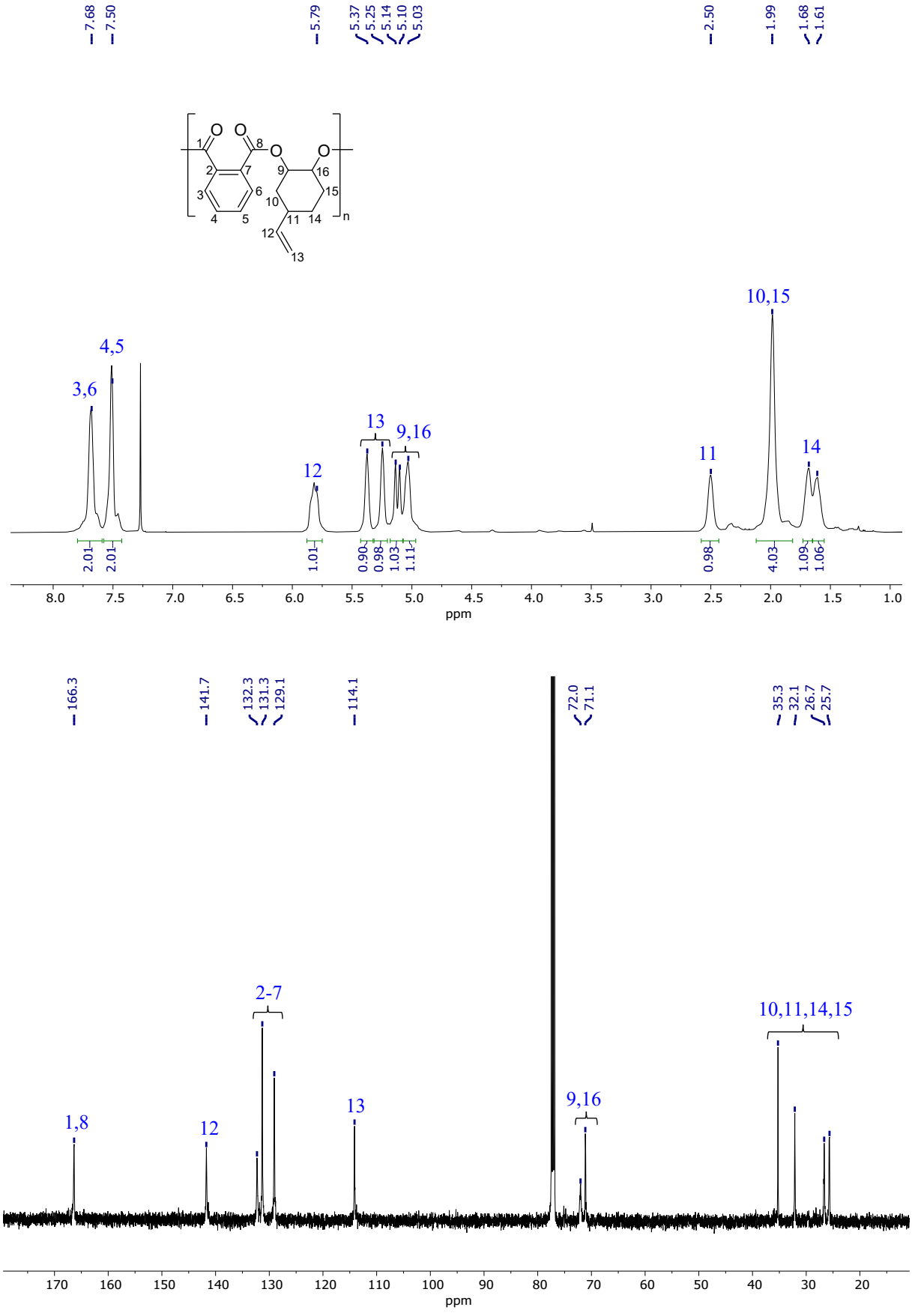

Figure S15. IR spectrum of poly(VCHO-*alt*-PA)

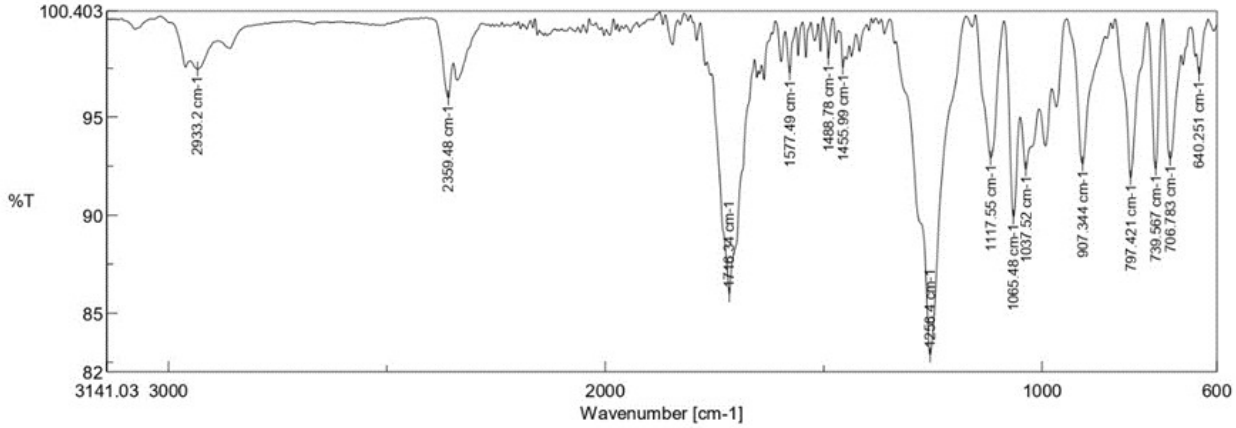

Figure S16. NMR spectra (500 MHz, $CDCl_3$, 298 K) of poly(VCHO-*alt*-CA)

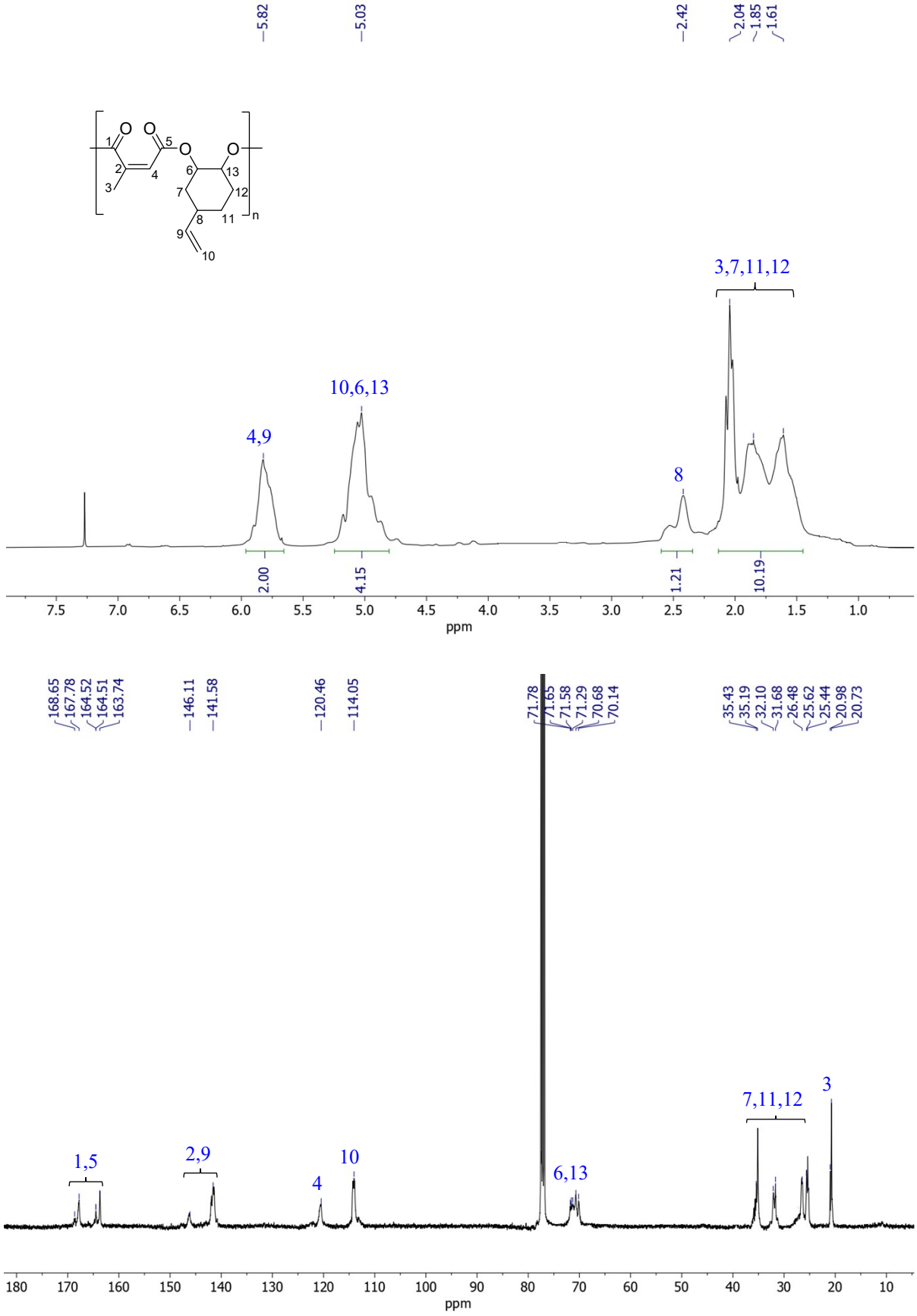

Figure S17. IR spectrum of poly(VCHO-*alt*-CA)

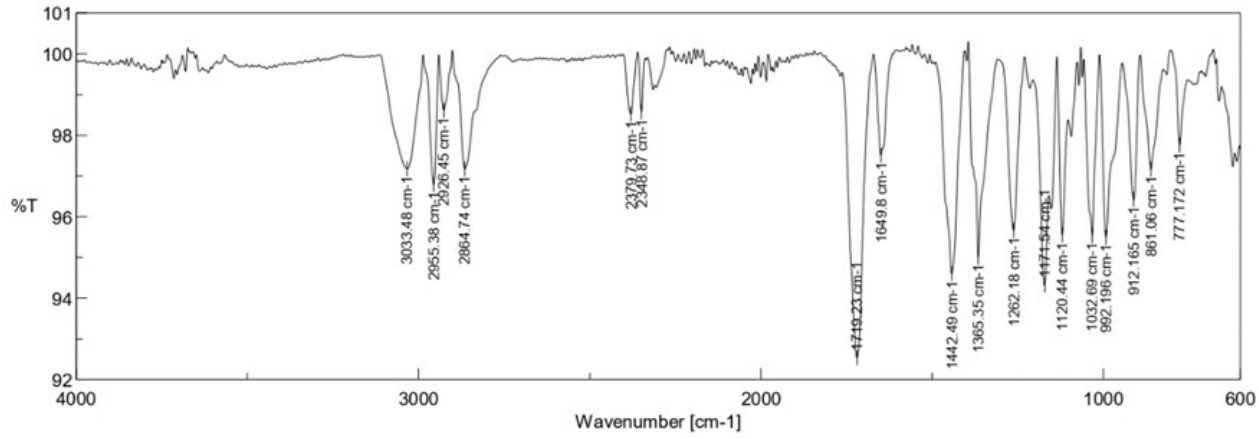

Figure S18. NMR spectra (500 MHz, $CDCl_3$, 298 K) of poly(MUO-*alt*-PA)

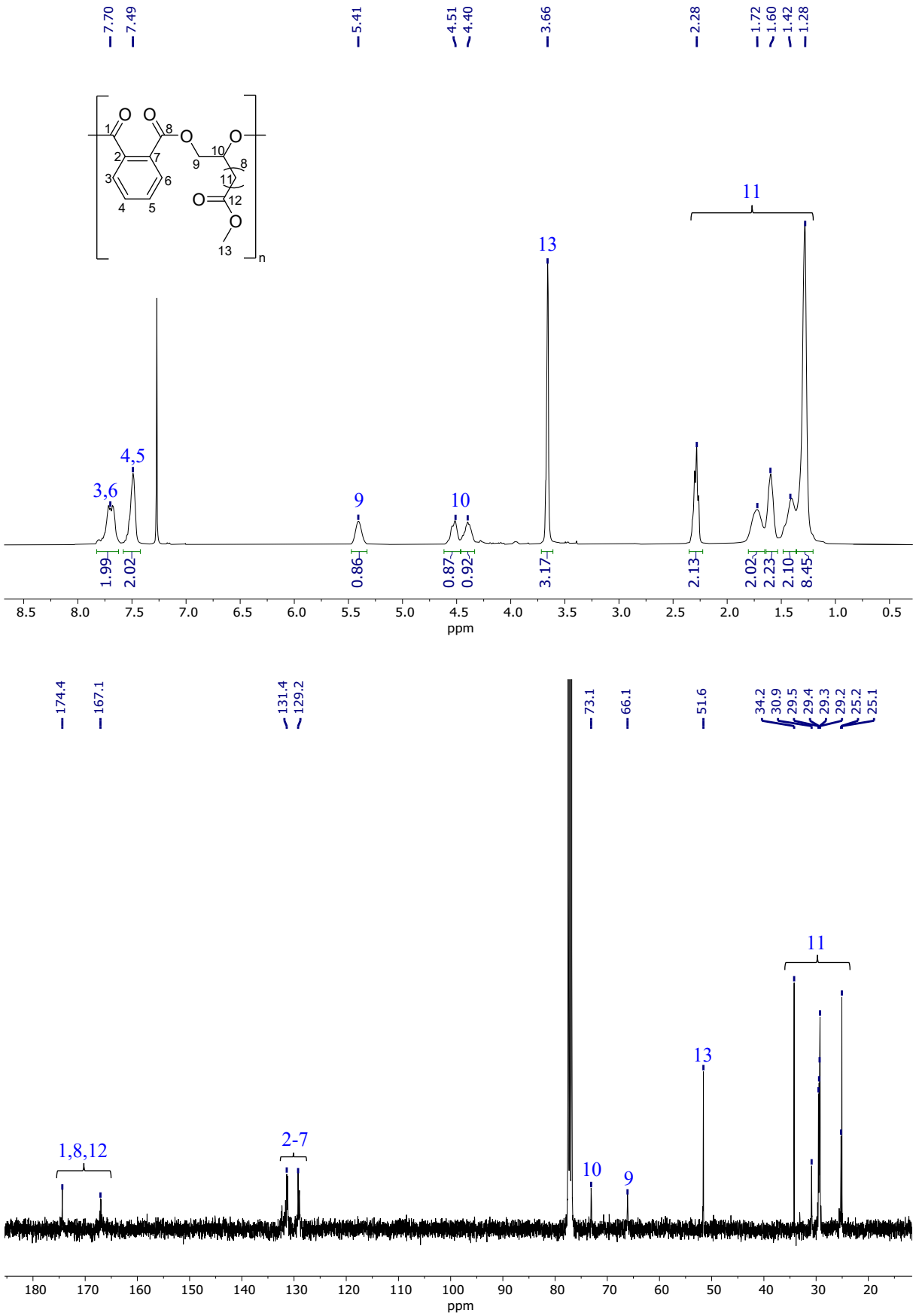

Figure S19. IR spectrum of poly(MUO-*alt*-PA)

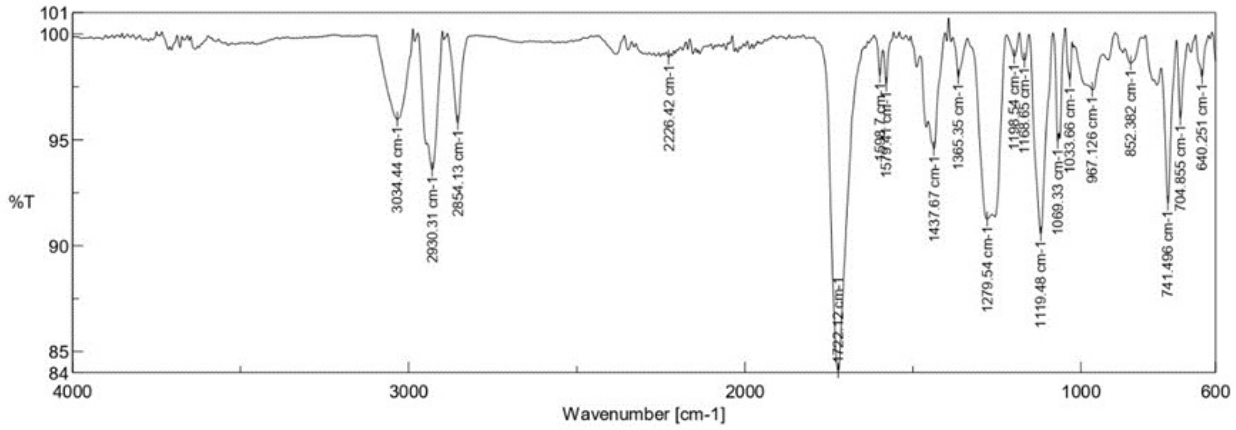

Figure S20. NMR spectra (500 MHz, $CDCl_3$, 298 K) of poly(MUO-*alt*-CA)

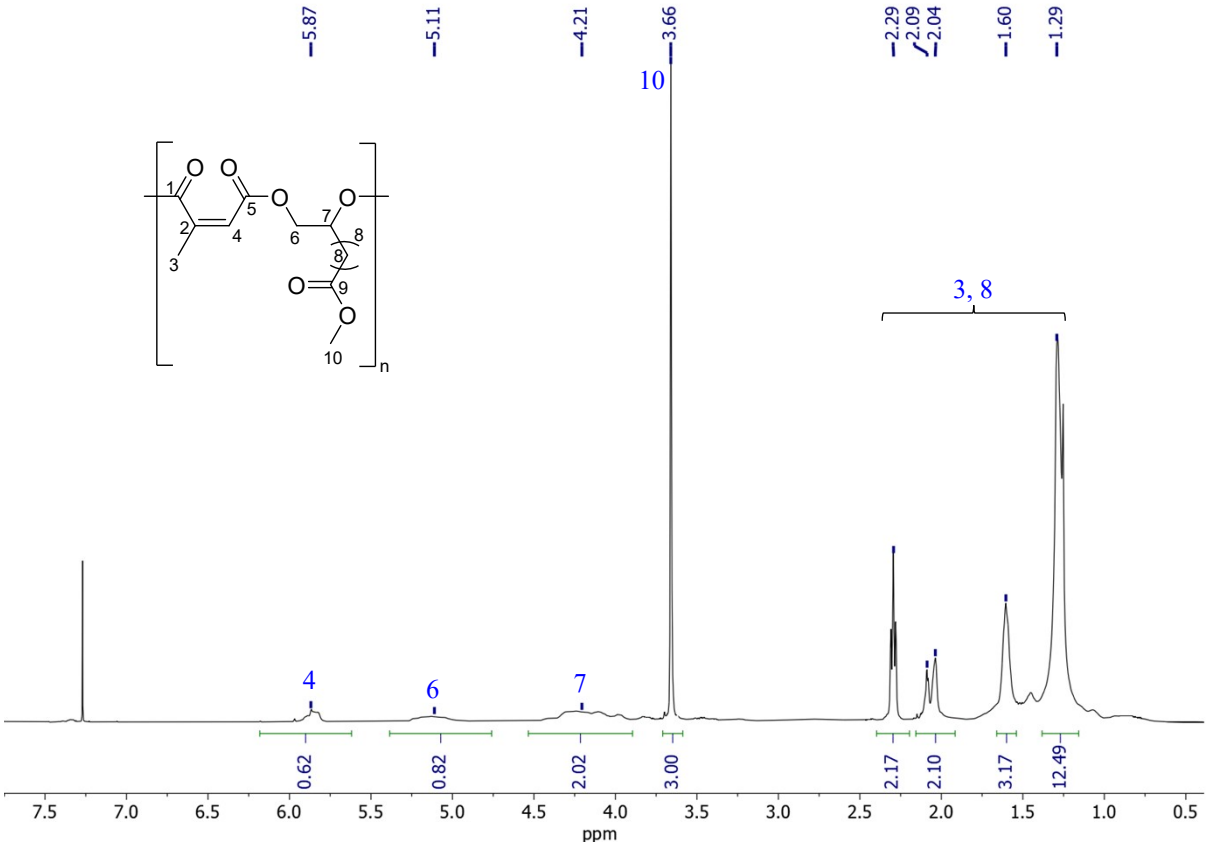

Figure S21. IR spectrum of poly(MUO-*alt*-CA)

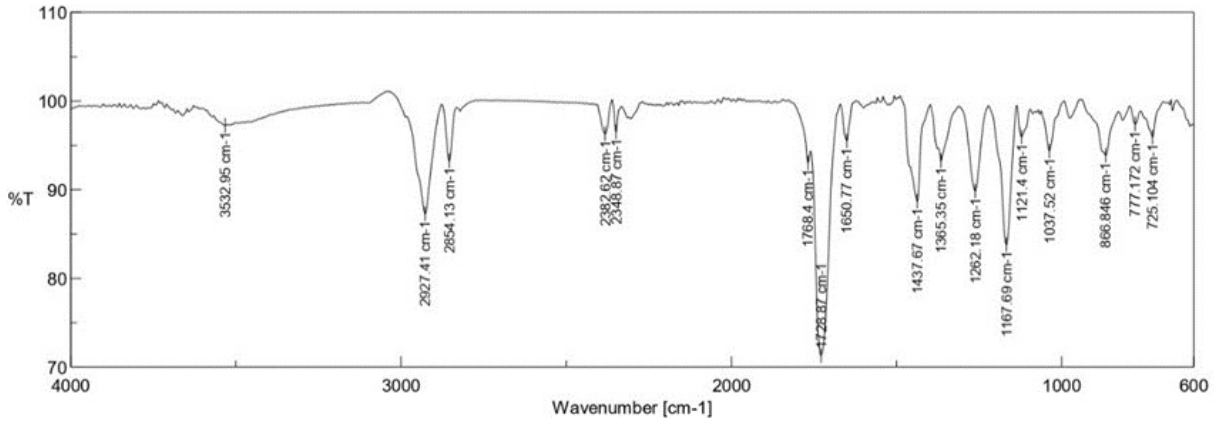

Figure S22. MALDI-ToF spectrum of poly(CHO-*alt*-PA) by catalyst **4**

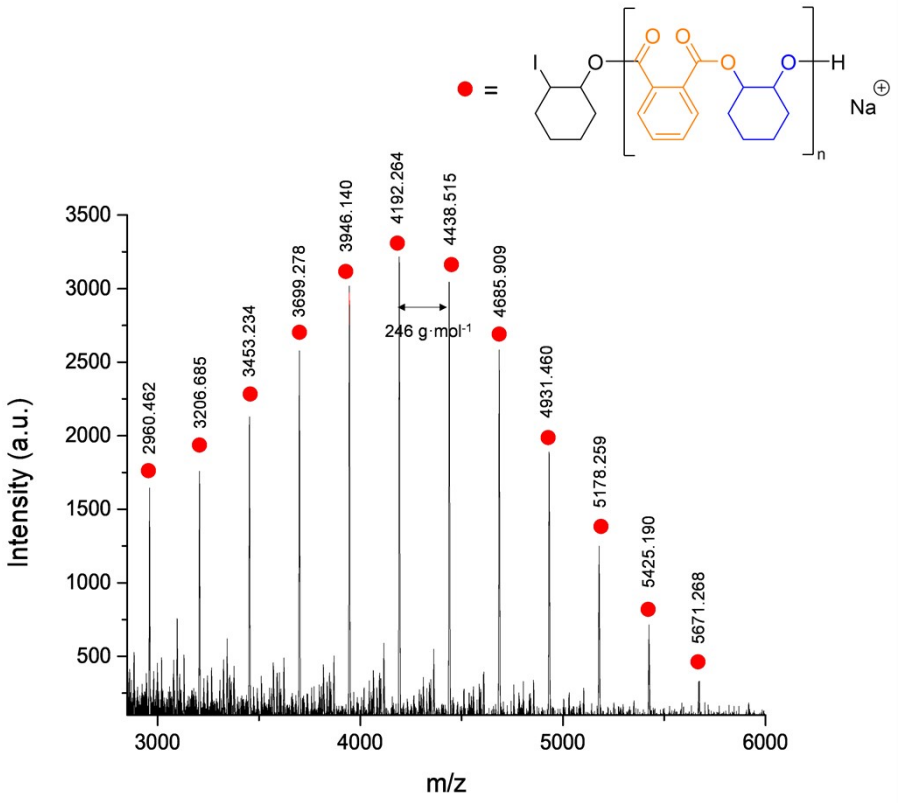

Figure S23. MALDI-ToF spectrum of poly(MUO-*alt*-PA) by catalyst **4**

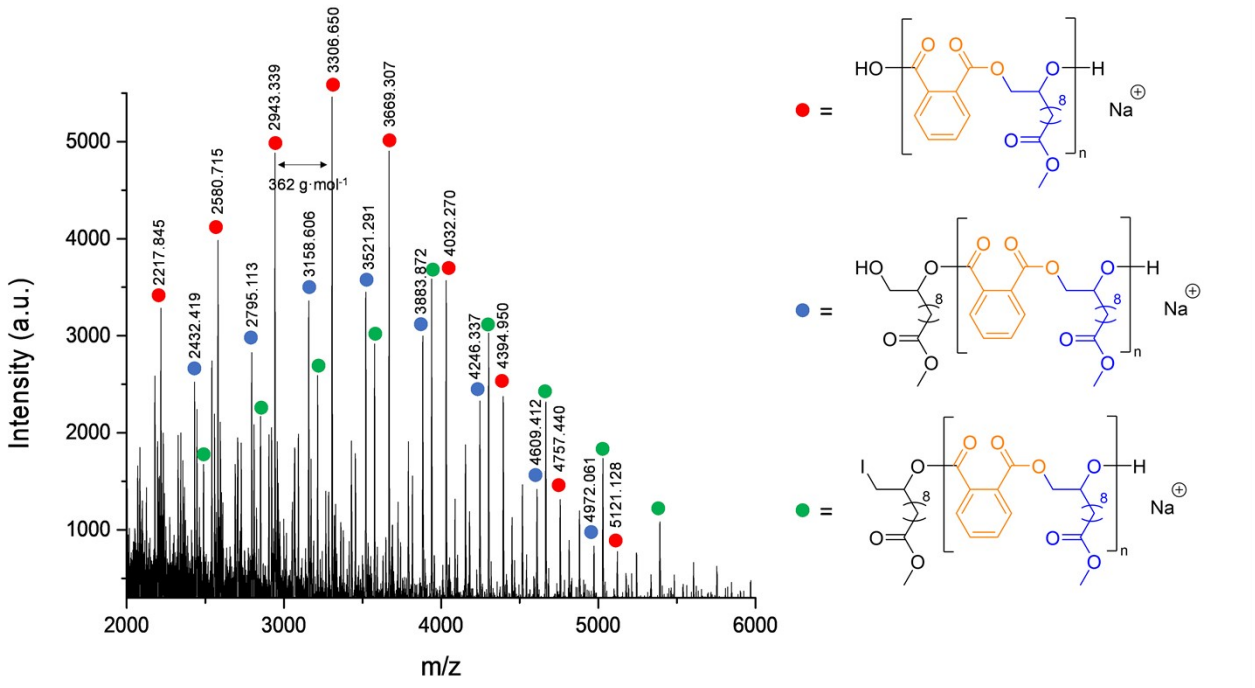

Figure S24. TGA analysis of poly(CHO-*alt*-PA)

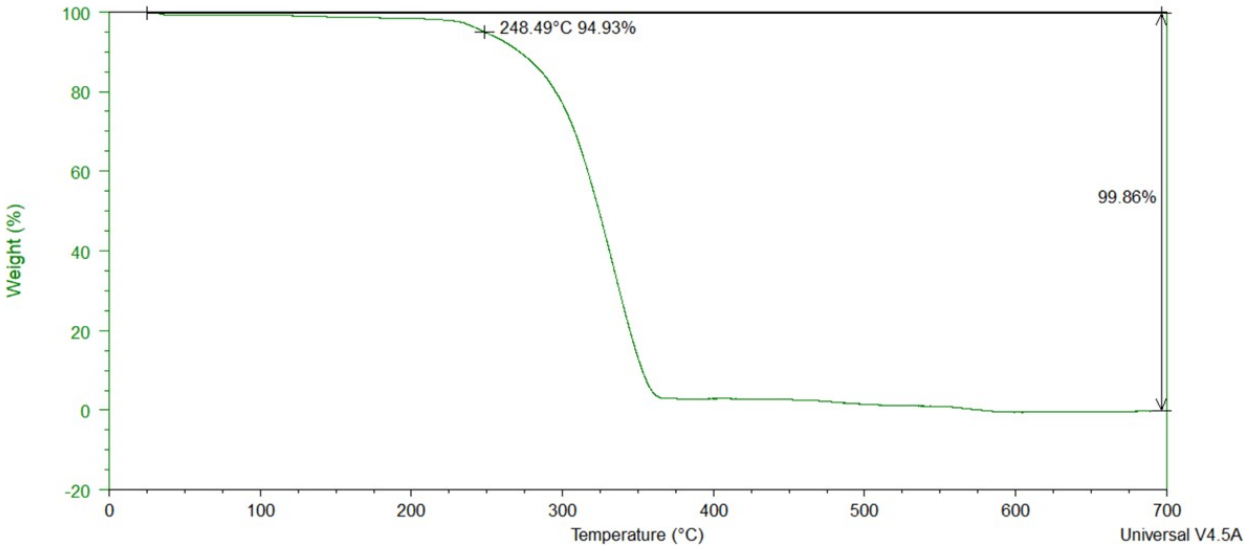

Figure S25. DSC analysis of poly(CHO-*alt*-PA)

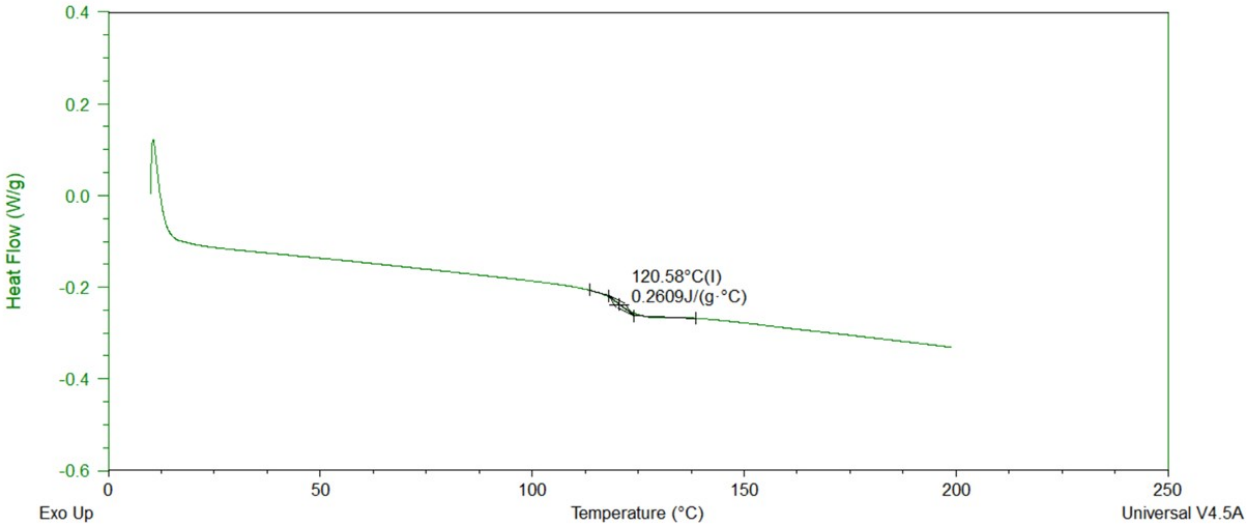

Figure S26. TGA analysis of poly(CHO-*alt*-CA)

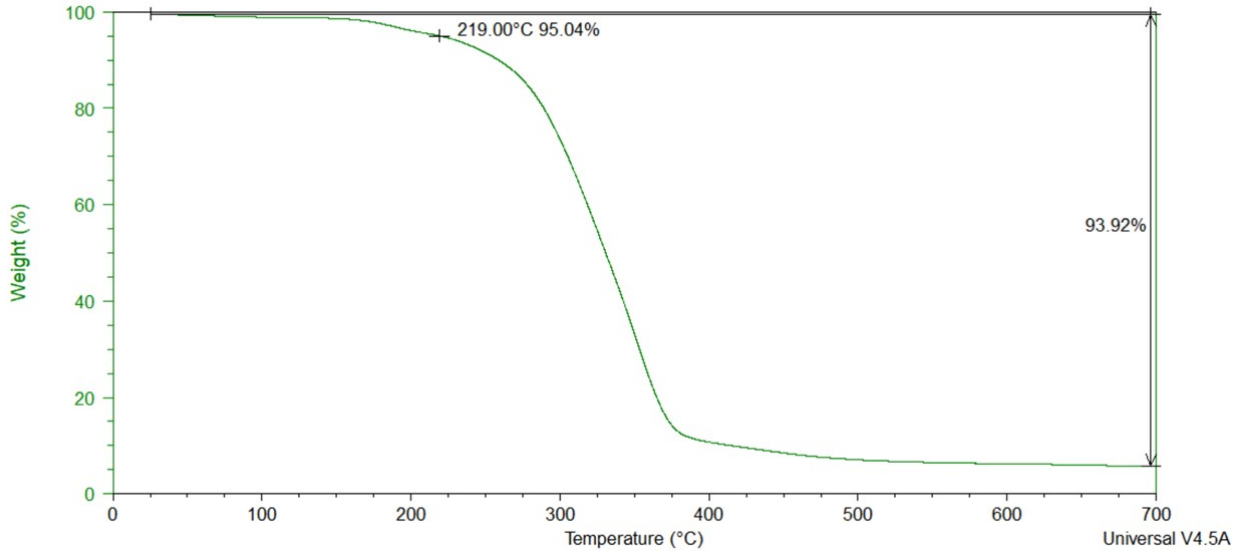

Figure S27. DSC analysis of poly(CHO-*alt*-PA)

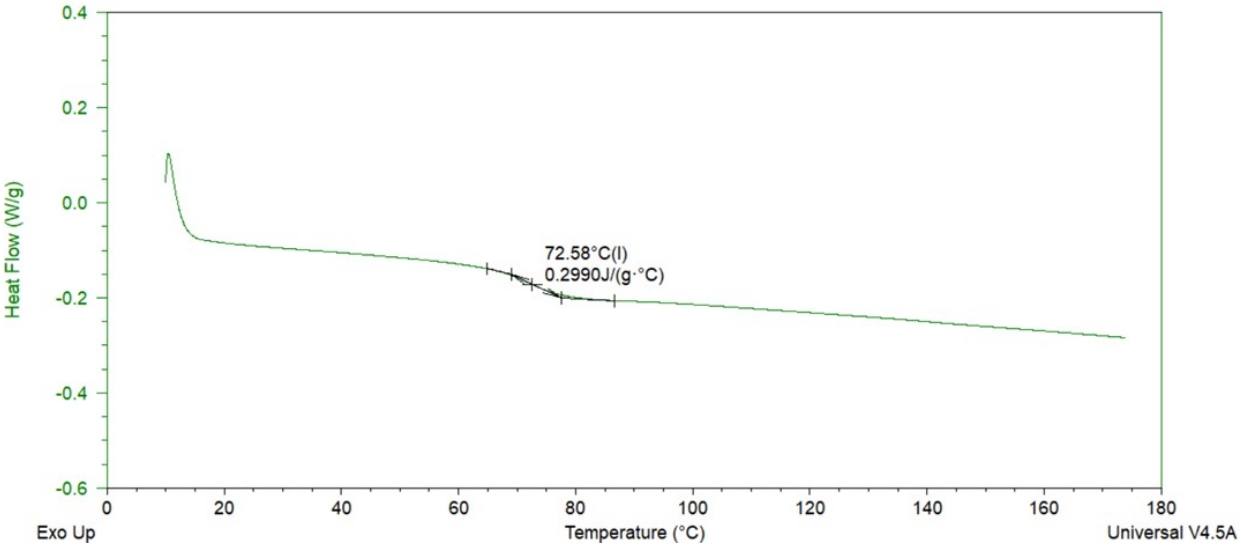

Figure S28. TGA analysis of poly(VCHO-*alt*-PA)

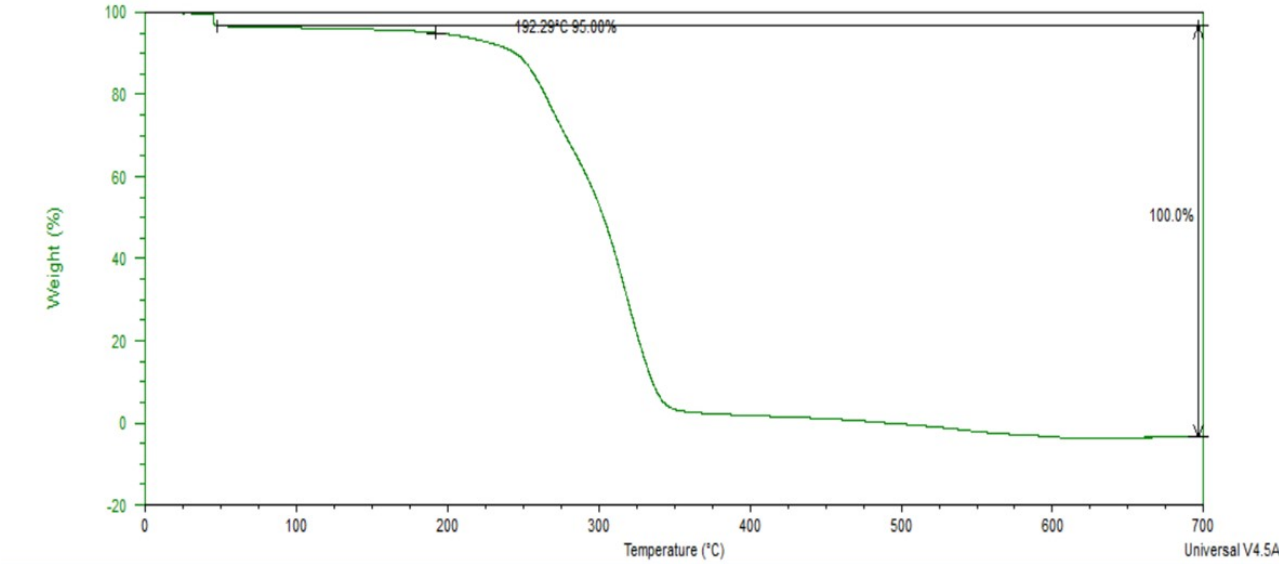

Figure S29. DSC analysis of poly(VCHO-*alt*-PA)

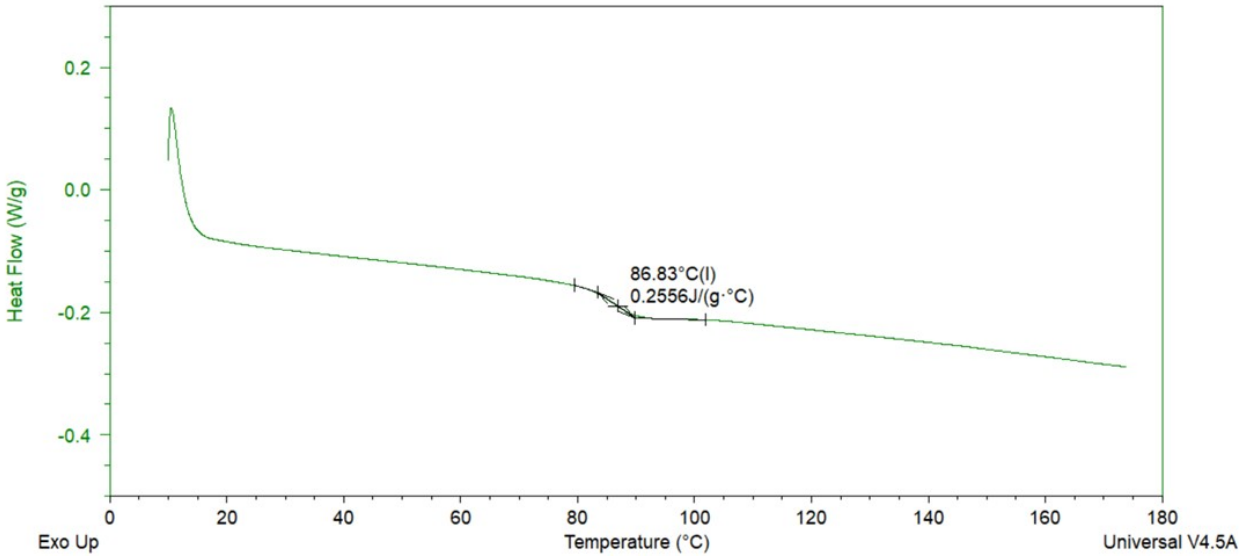

Figure S30. TGA analysis of poly(VCHO-*alt*-CA)

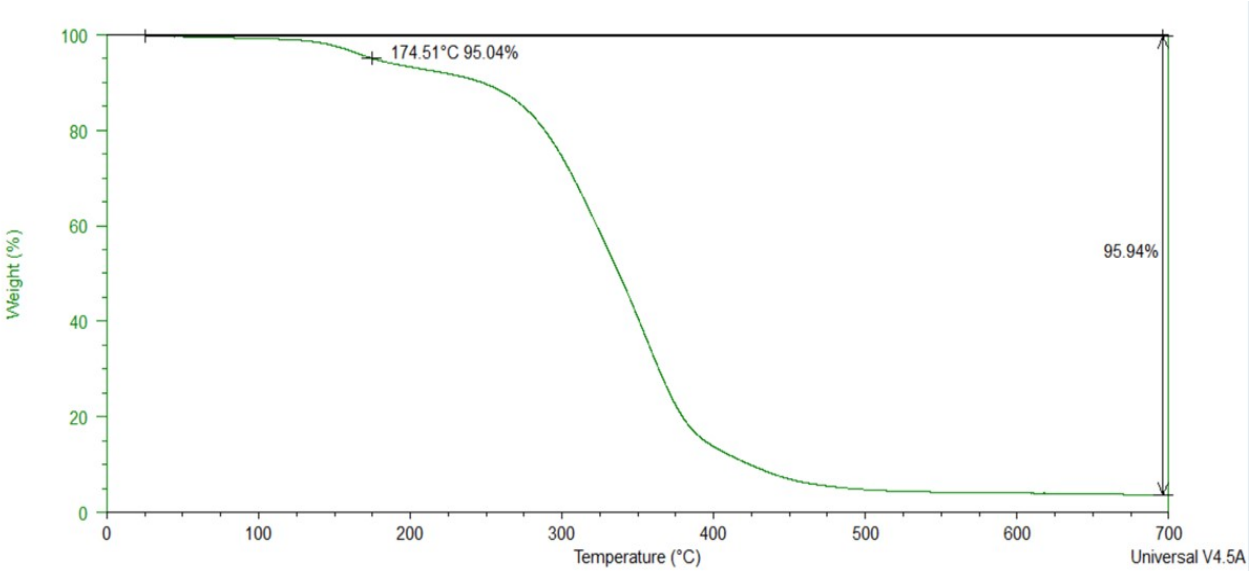

Figure S31. DSC analysis of poly(VCHO-*alt*-CA)

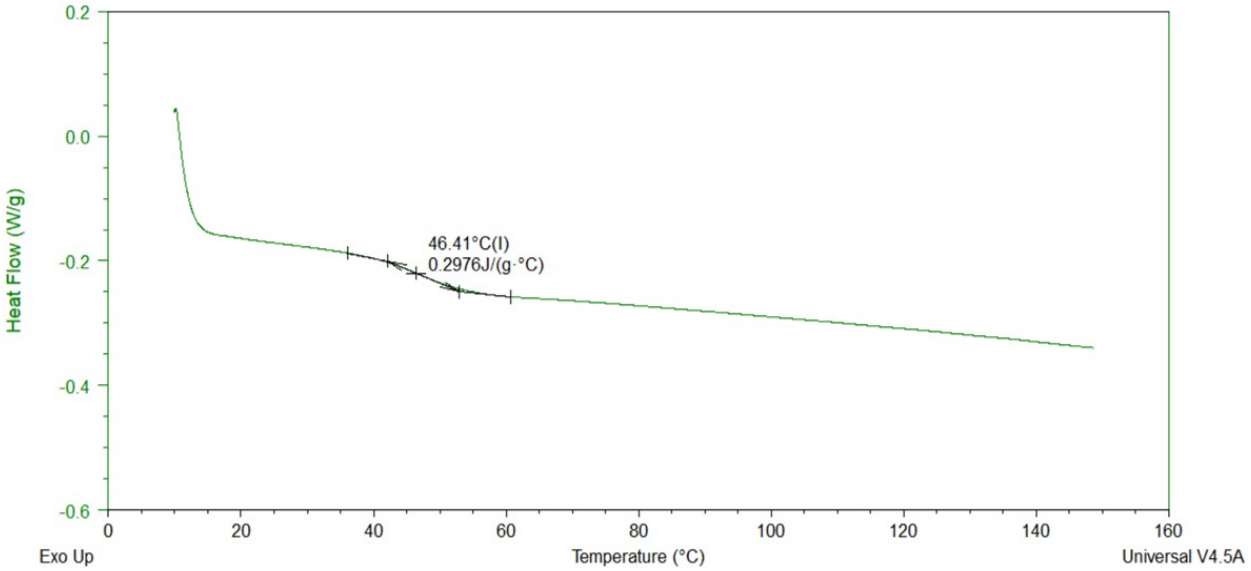

Figure S32. DSC analysis of poly(MUO-*alt*-PA)

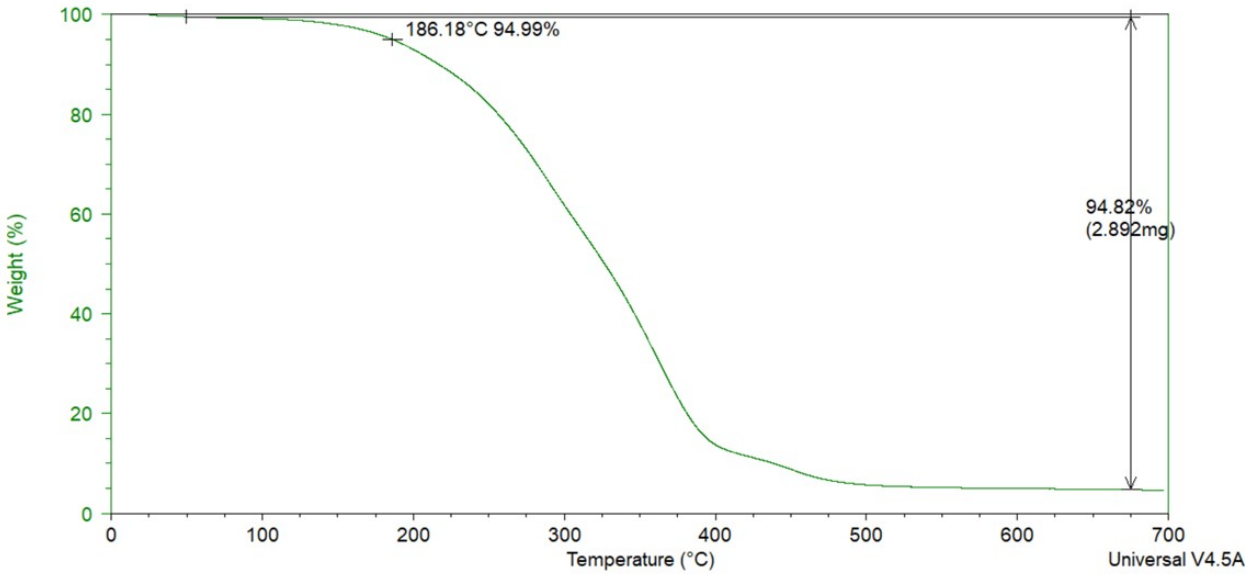

Figure S33. DSC analysis of poly(MUO-*alt*-CA)

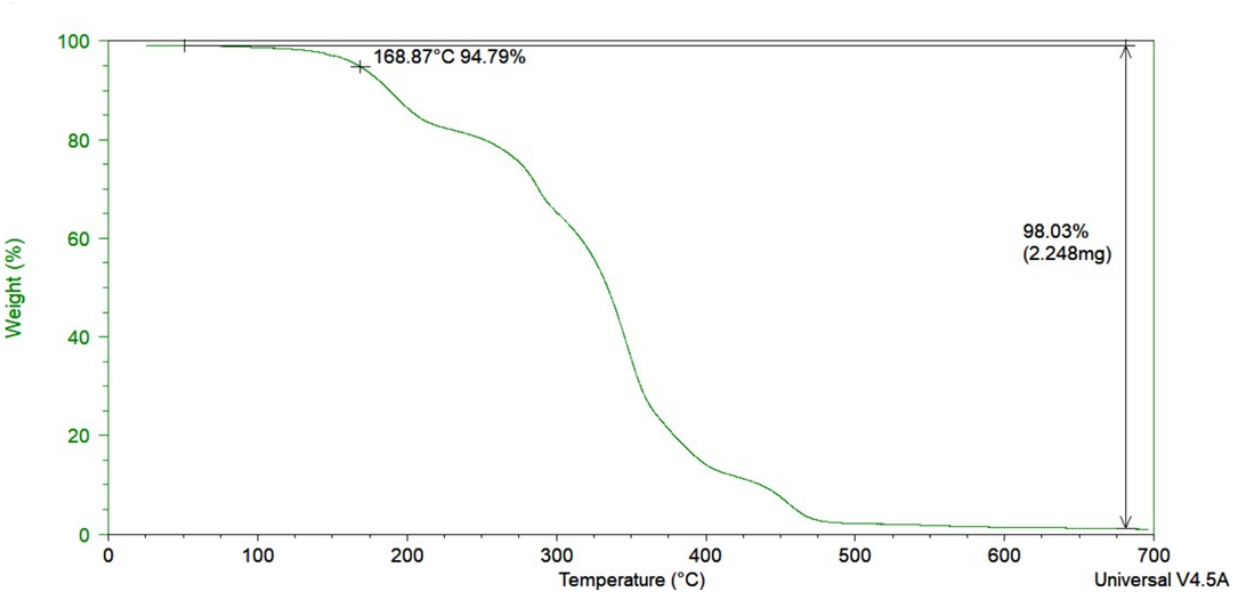

Table S5. Experimental data for kinetic polymerisation experiments.

Entry	[4] (M)	[CHO] (M)	[PA] (M)	Initial rate ($\times 10^{-5}$ M·s^{-1})
1	0.017	1.69	1.69	3.2
2	0.017	3.38	1.69	3.6
3	0.017	5.06	1.69	2.8
4	0.017	6.75	1.69	3.1
5	0.017	8.44	1.69	3.0
6	0.017	8.44	0.84	1.5
7	0.017	8.44	1.28	2.4
8	0.017	8.44	3.40	5.8
9	0.026	2.55	2.55	3.2
10	0.051	2.55	2.55	4.3
11	0.077	2.55	2.55	5.3
12	0.102	2.55	2.55	6.0
13	0.128	2.55	2.55	7.0

Figure S34. Overlay of plots of the formation of [poly(CHO-*alt*-PA)] versus time varying CHO concentrations (Table S5, entries 1–5). Initial rates are determined from the slope of the linear fitting and correspond to 0–20 % conversion.

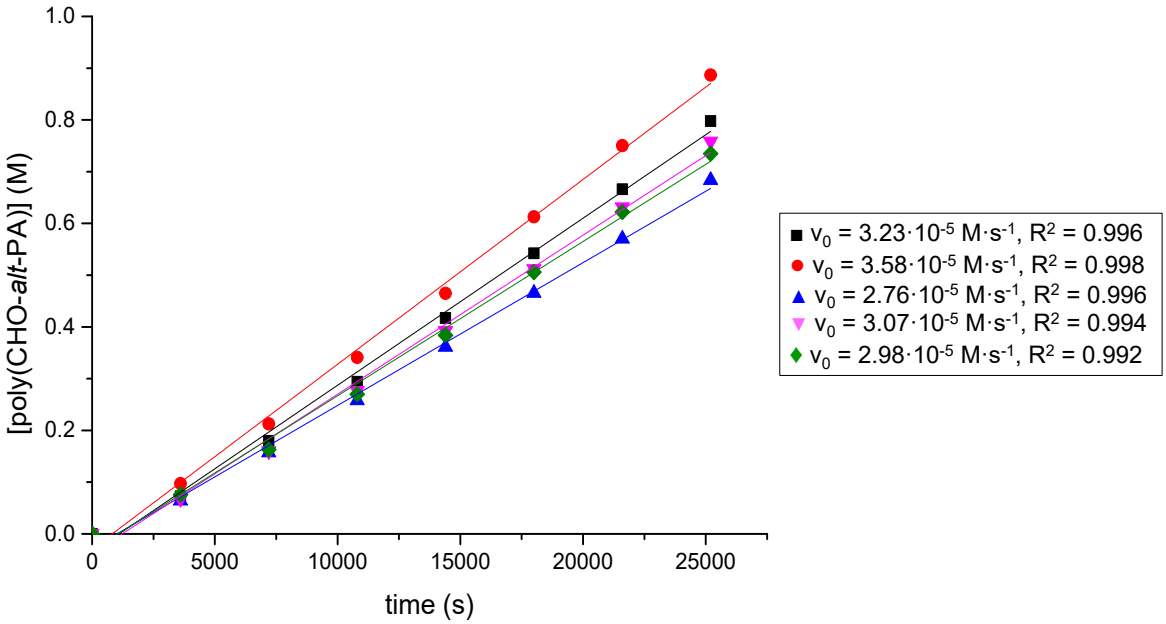

Figure S35. Overlay of plots of the formation of [poly(CHO-*alt*-PA)] versus time varying PA concentrations (Table S5, entries 5–8). Initial rates are determined from the slope of the linear fitting and correspond to 0–20 % conversion.

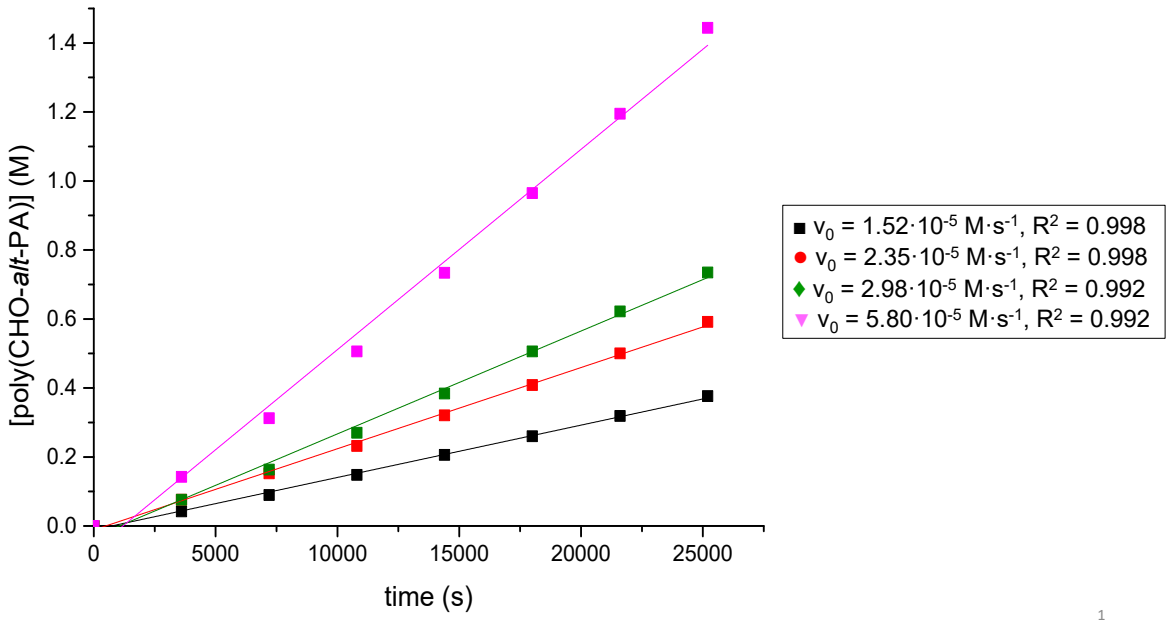

Figure S36. Overlay of plots of the formation of [poly(CHO-*alt*-PA)] versus time varying catalyst **4** concentrations (Table S5, entries 9–13). Initial rates are determined from the slope of the linear fitting and correspond to 0–20 % conversion.

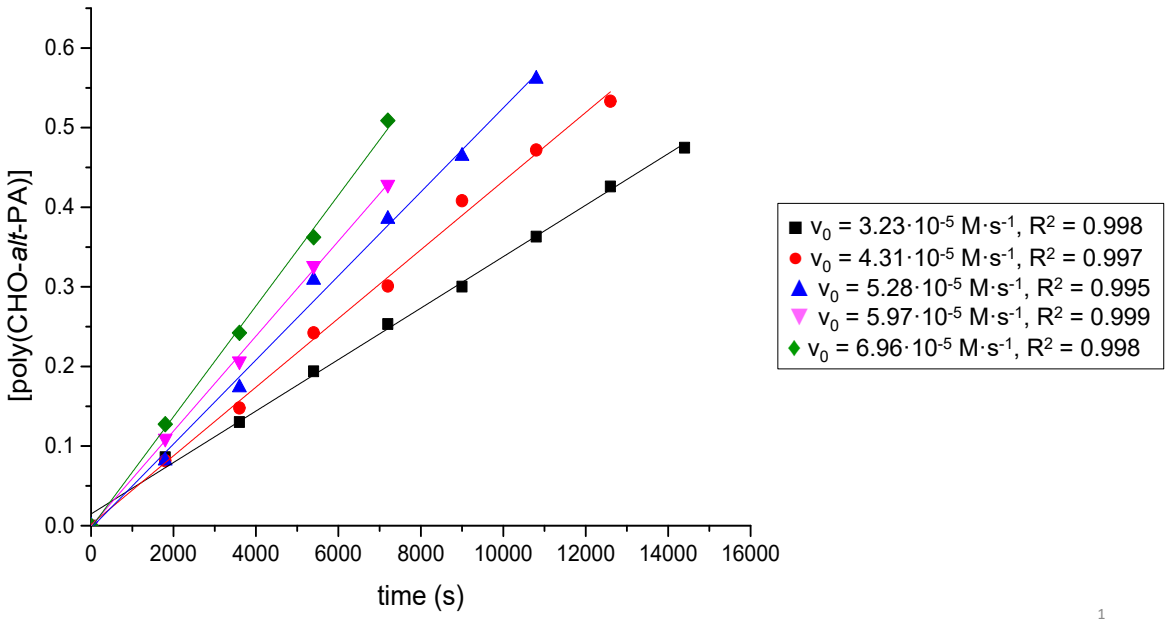

Figure S37. Plot of $\ln([PA]_t/[PA]_0)$ versus time varying catalyst **4** concentrations (Table S5, entries 9–13), revealing a linear relationship and hence confirming a first-order dependence of the rate on [PA].

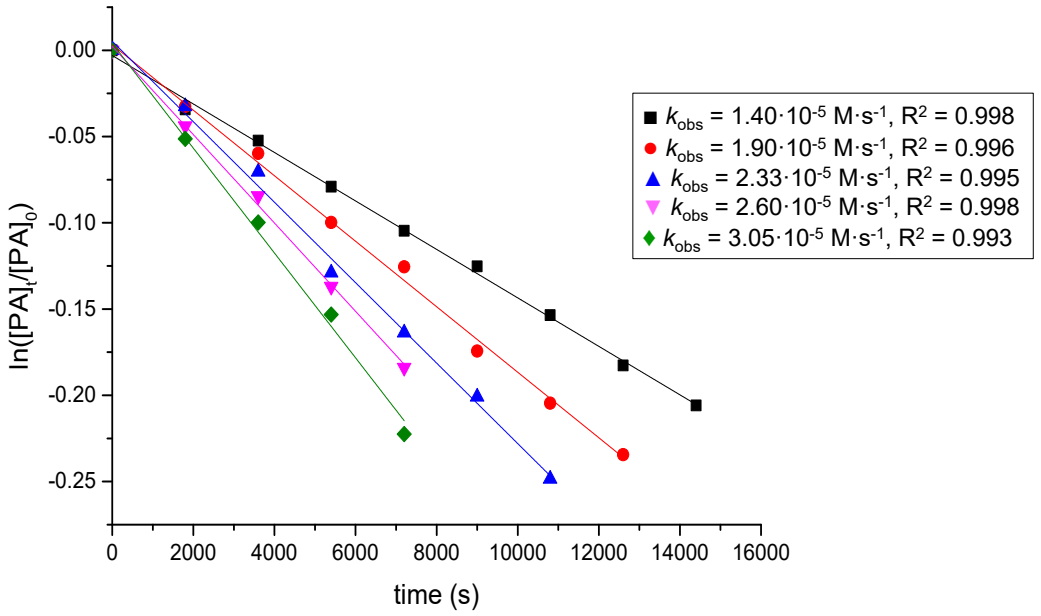

Figure S38. DOSY NMR analysis (500 MHz, d_8-THF, 298 K) of compound **4**.

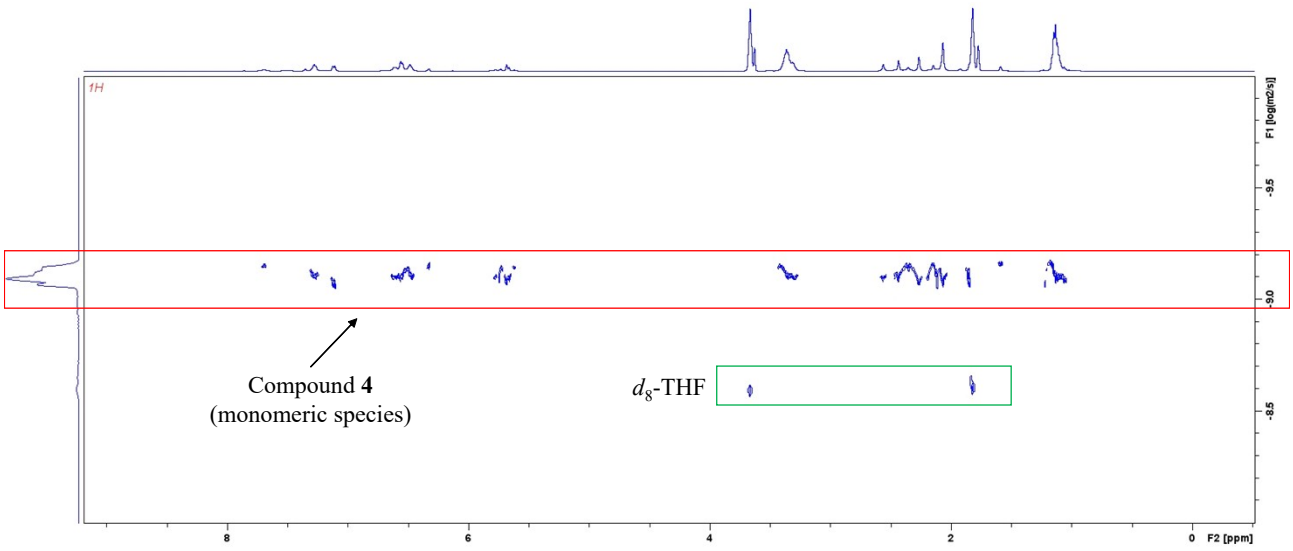

3. References

(1) Otero, A.; Fernández-Baeza, J.; Tejeda, J.; Lara-Sánchez, A.; Sánchez-Molina, M.; Franco, S.; López-Solera, I.; Rodríguez, A. M.; Sánchez-Barba, L. F.; Morante-Zarcero, S.; Garcés, A. *Inorg. Chem.* **2009**, *48*, 5540−5554; b) de la Cruz-Martínez, F.; Martínez, J.; Gaona, M. A.; Fernández-Baeza, J.; Sánchez-Barba, L. F.; Rodríguez, A. M.; Castro-Osma, J. A.; Otero, A.; Lara-Sánchez, A. *ACS Sustainable Chem. Eng.* **2018**, *6*, 5322−5332.

(2) Martínez, J.; de la Cruz-Martínez, F.; Martínez de Sarasa Buchaca, M.; Fernández-Baeza, J.; Sánchez-Barba, L. F.; North, M.; Castro-Osma, J. A.; Lara-Sánchez, A. *ChemPlusChem* **2021**, *86*, 460−468.

(3) Thevenon, A.; Cyriac, A.; Myers, D.; White, A. J. P.; Durr, C. B.; Williams, C. K. *J. Am. Chem. Soc.* **2018**, *140*, 6893−6903.

(4) de la Cruz-Martínez, F.; Martínez de Sarasa Buchaca, M.; Martínez, J.; Tejeda, J.; Fernández-Baeza, J.; Alonso-Moreno, C.; Rodríguez, A. M.; Castro-Osma, J. A.; Lara-Sánchez, A. *Inorg. Chem.* **2020**, *59*, 8412−8423.

(5) Fieser, M. E.; Sanford, M. J.; Mitchell, L. A.; Dunbar, C. R.; Mandal, M.; Van Zee, N. J.; Urness, D. M.; Cramer, C. J.; Coates, G. W.; Tolman, W. B. *J. Am. Chem. Soc.* **2017**, *139*, 15222−15231.

(6) a) Sheldrick, G. M. *Acta Cryst. C*, **2015**, *71*, 3–8; b) Sheldrick, G. M. *Acta Cryst. A*, **2015**, *71*, 3–8.

(7) Dolomanov, O. V.; Bourhis, L. J.; Gildea, R. J.; Howard, J. A. K. K.; Puschmann, H. *J. Appl. Cryst.* **2009**, *42*, 339–341.